University of Denver
Digital Commons @ DU

Electronic Theses and Dissertations Graduate Studies

8-2023

Consensus-Based Active and Reactive Power Control and Management of Microgrids

Shruti Singh
University of Denver

Follow this and additional works at: https://digitalcommons.du.edu/etd

Part of the Other Electrical and Computer Engineering Commons, and the Power and Energy Commons

Recommended Citation

Singh, Shruti, "Consensus-Based Active and Reactive Power Control and Management of Microgrids" (2023). *Electronic Theses and Dissertations*. 2318.
https://digitalcommons.du.edu/etd/2318

All Rights Reserved
All Rights Reserved.
This Dissertation is brought to you for free and open access by the Graduate Studies at Digital Commons @ DU. It has been accepted for inclusion in Electronic Theses and Dissertations by an authorized administrator of Digital Commons @ DU. For more information, please contact jennifer.cox@du.edu,dig-commons@du.edu.

Consensus-Based Active and Reactive Power Control and Management of Microgrids

Abstract

Microgrids incorporating distributed generation and renewable energy sources offer potential solutions to the energy crisis while modernizing traditional grids. Despite cost-effectiveness in some technologies, financial support remains crucial for expensive ones like PV, fuel cells, and storage technologies. Microgrids bring economic benefits, efficiency, reduced emissions, and improved power quality. Their success hinges on cost reductions in renewables, storage, reliability, and energy management systems, enabling operation both with and without the utility grid.

Economic Dispatch optimizes system costs, considering all constraints. Various methods tackle this problem, including quadratic convex functions, Lagrangian relaxation, and quadratic programming. For microgrids with distributed generators, seamless communication and secure operation are vital. This dissertation addresses the inclusion of noise as a constraint in grid-connected and islanded microgrids, aiming to enhance economic dispatch solutions and overall performance. A virtual synchronous generator control strategy improves power quality, employing a noiseless consensus-based algorithm. Reactive power management utilizes a STATCOM controller to enhance voltage, output power, and phase angle stability. Three algorithms—Lagrange, Firefly, and Artificial Bee Colony—are studied for active and reactive power compensation with and without the VSG-STATCOM strategy at various noise levels.

The dissertation also presents findings from a NREL-funded project on Cost analysis of microgrids in the U.S. The study identifies average costs for typical microgrid projects over the next five years, aiding future R&D and project planning for investors, developers, and researchers. Data analysis focuses on commercial, community, and campus microgrid sectors to derive meaningful insights. Ultimately, microgrids with distributed generation and renewable sources hold promise for a more sustainable and resilient energy future.

Document Type

Dissertation

Degree Name

Ph.D.

First Advisor

David Wenzhong Gao

Second Advisor

Amin Khodaei

Third Advisor

Mohammad Matin

Keywords

Microgrids, Renewable energy, Energy crisis, Cost

Subject Categories

Electrical and Computer Engineering | Engineering | Other Electrical and Computer Engineering | Power and Energy

Publication Statement

Copyright is held by the author. User is responsible for all copyright compliance.

This dissertation is available at Digital Commons @ DU: https://digitalcommons.du.edu/etd/2318

CONSENSUS-BASED ACTIVE AND REACTIVE POWER CONTROL & MANAGEMENT OF MICROGRIDS

A Dissertation

Presented to

the Faculty of the Daniel Felix Ritchie School of Engineering and Computer Science

University of Denver

In Partial Fulfillment

of the Requirements for the Degree

Doctor of Philosophy

by

Shruti Singh

August 2023

Advisor: Dr. David Wenzhong Gao

©Copyright by Shruti Singh 2023

All Rights Reserved

Author: Shruti Singh
Title: CONSENSUS-BASED ACTIVE AND REACTIVE POWER CONTROL & MANAGEMENT OF MICROGRIDS
Advisor: Dr. David Wenzhong Gao
Degree Date: August 2023

Abstract

Microgrids incorporating distributed generation and renewable energy sources offer potential solutions to the energy crisis while modernizing traditional grids. Despite cost-effectiveness in some technologies, financial support remains crucial for expensive ones like PV, fuel cells, and storage technologies. Microgrids bring economic benefits, efficiency, reduced emissions, and improved power quality. Their success hinges on cost reductions in renewables, storage, reliability, and energy management systems, enabling operation both with and without the utility grid.

Economic Dispatch optimizes system costs, considering all constraints. Various methods tackle this problem, including quadratic convex functions, Lagrangian relaxation, and quadratic programming. For microgrids with distributed generators, seamless communication and secure operation are vital. This dissertation addresses the inclusion of noise as a constraint in grid-connected and islanded microgrids, aiming to enhance economic dispatch solutions and overall performance. A virtual synchronous generator control strategy improves power quality, employing a noiseless consensus-based algorithm. Reactive power management utilizes a STATCOM controller to enhance voltage, output power, and phase angle stability. Three algorithms—Lagrange, Firefly, and Artificial Bee Colony—are studied for active and reactive power compensation with and without the VSG-STATCOM strategy at various noise levels.

The dissertation also presents findings from a NREL-funded project on Cost analysis of microgrids in the U.S. The study identifies average costs for typical microgrid projects over the next five years, aiding future R&D and project planning for investors, developers, and researchers. Data analysis focuses on commercial, community, and campus microgrid sectors to derive meaningful insights. Ultimately, microgrids with distributed generation and renewable sources hold promise for a more sustainable and resilient energy future.

Acknowledgements

I would like to express my sincere gratitude to my advisor and Chair of the Department of Electrical and Computer Engineering at University of Denver, Dr. David Wenzhong Gao. Since my first day in graduate school, Dr. Gao provided me endless support, guidance, and encouragement. I am truly grateful for all his support and considerations.

I thank my parents, husband, and brother for their unlimited support and persuasion. I’m also grateful to my son for his patience and understanding during this time. I would like to express my deepest gratitude to them for all their sacrifices, encouragements, and best wishes throughout my life.

Table of Contents

Abstract ii

Acknowledgements ivii

List of Figures vii

List of Tables x

Chapter 1. Introduction 1

Chapter 2. Literature Review 4
  2.1 Existing Methods 4
    2.1.1 Importance of Grid-connected Microgrids 7
    2.1.2 Importance of Islanded Microgrids 10
    2.1.3 Existing Microgrid Control & Management methods……………......13
  2.2 Research motivation ……………………………..…………………………15

Chapter 3. Economic Dispatch and Consensus based algorithm 17
  3.1 Problem Formulation for Economic Dispatch 17
    3.1.1 Lagrange Method..………………………………………………...17
    3.1.2 Particle Swarm Optimization 19
    3.1.3 Firefly Algorithm 20
    3.1.4 Artificial Bee Colony Algorithm 22
  3.2 Consensus-based Economic Dispatch for noiseless communication 24
  3.3 Numerical Simulations 28
  3.4 Discussions 33

Chapter 4. Control Strategies 35
  4.1 Virtual Synchronous Generator 35
    4.1.1 Numerical Simulations 41
  4.2 Reactive Power Compensation and STATCOM controller 47
    4.2.1 Numerical Simulations 51
  4.3 Network figure and single line diagram of system…………………………..56
  4.4 Discussions 58

Chapter 5. Comparison results of different algorithms…………………………………60
  5.1 Comparison between Lagrange Method and PSO algorithms………………60
  5.2 Comparison between Lagrange, Firefly and ABC algorithms………………62
  5.3 Discussions…………………………………………………………………..72

Chapter 6. Cost study of Microgrids 75
  6.1 Importance of cost study 76
    6.1.1 Histogram and Principal Component Analysis 77
  6.2 Discussions 86

Chapter 7. Research Conclusion and Future Work.. 87
    7.1 Conclusion 87
    7.2 Future research.. 88

List of Publications 89

References... 90

Appendix... 106

List of Figures

Chapter 3

FIGURE 3.1 FLOWCHART FOR ED SOLUTION USING FA 22
FIGURE 3.2 ALGORITHM FLOWCHART 28
FIGURE 3.3 OUTPUT POWER OF GENERATOR UNITS IN KW WITHOUT NOISE 30
FIGURE 3.4 OUTPUT POWER OF GENERATOR UNITS IN KW WITH 0.2 NOISE VARIANCE 30
FIGURE 3.5 OUTPUT POWER OF GENERATOR UNITS IN KW WITH 0.5 NOISE VARIANCE 30
FIGURE 3.6 OUTPUT POWER OF GENERATOR UNITS IN KW WITH 0.8 NOISE VARIANCE 31
FIGURE 3.7 INCREMENTAL COST (IC) OF GENERATOR UNITS WITHOUT NOISE 32
FIGURE 3.8 INCREMENTAL COST (IC) OF GENERATOR UNITS WITH 0.2 NOISE VARIANCE ... 32
FIGURE 3.9 INCREMENTAL COST (IC) OF GENERATOR UNITS WITH 0.5 NOISE VARIANCE ... 32
FIGURE 3.10 INCREMENTAL COST (IC) OF GENERATOR UNITS WITH 0.8 NOISE VARIANCE . 33

Chapter 4

FIGURE 4.1 VSG CONTROL STRATEGY BLOCK DIAGRAM 36
FIGURE 4.2 STATOR VOLTAGE MODEL 37
FIGURE 4.3 ROTOR MOTION MODEL 38
FIGURE 4.4 FREQUENCY REGULATION MODULE 38
FIGURE 4.5 VOLTAGE REGULATION MODULE 39
FIGURE 4.6 GRID CONTROL MODULE 40
FIGURE 4.7 OUTPUT POWER OF GENERATOR UNITS IN KW WITHOUT NOISE AND VSG 42
FIGURE 4.8 OUTPUT POWER OF GENERATOR UNITS IN KW WITHOUT NOISE WITH VSG 42
FIGURE 4.9 OUTPUT POWER OF GENERATOR UNITS IN KW WITH 0.2 NOISE VARIANCE WITHOUT VSG 43
FIGURE 4.10 OUTPUT POWER OF GENERATOR UNITS IN KW WITH 0.5 NOISE VARIANCE WITHOUT VSG 43
FIGURE 4.11 OUTPUT POWER OF GENERATOR UNITS IN KW WITH 0.8 NOISE VARIANCE WITHOUT VSG 44
FIGURE 4.12 OUTPUT POWER OF GENERATOR UNITS IN KW WITH ALL NOISE VARIANCE WITH VSG 44
FIGURE 4.13 COMPARISON OF FREQUENCY CHANGE OF GENERATOR UNITS WITH 0.8 NOISE VARIANCE WITHOUT VSG 45
FIGURE 4.14 COMPARISON OF FREQUENCY CHANGE OF GENERATOR UNITS WITH 0.8 NOISE VARIANCE WITH VSG 46
FIGURE 4.15 COMPARISON OF MAXIMUM POWER OF GENERATOR UNITS WITH 0.8 NOISE VARIANCE AND LOAD CHANGE WITHOUT VSG 46
FIGURE 4.16 COMPARISON OF MAXIMUM POWER OF GENERATOR UNITS WITH 0.8 NOISE VARIANCE AND LOAD CHANGE WITH VSG 46
FIGURE 4.17 TRANSFER FUNCTION MODEL OF STATCOM WITH PI CONTROLLER 48
FIGURE 4.18 MICROGRID STRUCTURE INCLUDING PV, WIND GENERATOR, STEAM TURBINE AND STATCOM CONTROLLER AS BUS INPUTS AND DELTA CONNECTED LOAD AS OUTPUT FROM THE BUS 49

FIGURE 4.19 COMPARISON OF TERMINAL VOLTAGE FOR ALL NOISE CONDITIONS 53
FIGURE 4.20 VOLTAGE FLUCTUATIONS FOR ALL NOISE VARIANCES WITH AND WITHOUT VSG 53
FIGURE 4.21 FREQUENCY FLUCTUATIONS FOR ALL NOISE VARIANCES WITH AND WITHOUT VSG 54
FIGURE 4.22 COMPARISON OF ACTIVE POWER FOR NO NOISE 54
FIGURE4.23 ACTIVE POWER FOR ALL NOISE VARIANCES WITH AND WITHOUT VSG 55
FIGURE 4.24 REACTIVE POWER FOR ALL NOISE VARIANCES WITH AND WITHOUT VSG 55
FIGURE 4.25 NETWORK FIGURE 57
FIGURE 4.26 SINGLE LINE DIAGRAM OF SYSTEM 58

Chapter 5

FIGURE 5.1 COMPARISON OF GENERATOR UNITS' OUTPUT POWER IN KW WITH 0.8 NOISE LEVEL FOR LAGRANGE AND PSO ALGORITHM USING VSG 60
FIGURE 5.2 COMPARISON OF INCREMENTAL COST OF UNITS USING LAGRANGE METHOD WITH VSG-STATCOM STRATEGY 63
FIGURE 5.3 COMPARISON OF INCREMENTAL COST OF UNITS USING FA ALGORITHM WITH VSG-STATCOM STRATEGY 63
FIGURE 5.4 COMPARISON OF INCREMENTAL COST OF UNITS USING ABC ALGORITHM WITH VSG-STATCOM STRATEGY 64
FIGURE 5.5 COMPARISON FOR VOLTAGE FLUCTUATIONS FOR NO NOISE WITH AND WITHOUT VSG 65
FIGURE 5.6 COMPARISON FOR VOLTAGE FLUCTUATIONS FOR 0.2 NOISE LEVEL WITH AND WITHOUT VSG 65
FIGURE 5.7 COMPARISON FOR VOLTAGE FLUCTUATIONS FOR 0.5 NOISE LEVEL WITH AND WITHOUT VSG 65
FIGURE 5.8 COMPARISON FOR VOLTAGE FLUCTUATIONS FOR 0.8 NOISE LEVEL WITH AND WITHOUT VSG 66
FIGURE 5.9 COMPARISON FOR FREQUENCY FLUCTUATIONS FOR NO NOISE CONDITION WITH AND WITHOUT VSG. 66
FIGURE 5.10 COMPARISON FOR FREQUENCY FLUCTUATIONS FOR 0.2 NOISE LEVEL WITH AND WITHOUT VSG 67
FIGURE 5.11 COMPARISON FOR FREQUENCY FLUCTUATIONS FOR 0.5 NOISE LEVEL WITH AND WITHOUT VSG 67
FIGURE 5.12 COMPARISON FOR FREQUENCY FLUCTUATIONS FOR 0.8 NOISE LEVEL WITH AND WITHOUT VSG 67
FIGURE 5.13 ACTIVE POWER FOR ALL NOISE VARIANCES WITH AND WITHOUT VSG FOR LAGRANGE METHOD 68
FIGURE 5.14 ACTIVE POWER FOR ALL NOISE VARIANCES WITH AND WITHOUT VSG FOR FIREFLY ALGORITHM 69
FIGURE 5.15 ACTIVE POWER FOR ALL NOISE VARIANCES WITH AND WITHOUT VSG FOR ABC ALGORITHM 69
FIGURE 5.16 REACTIVE POWER FOR ALL NOISE VARIANCES WITH AND WITHOUT VSG FOR LAGRANGE METHOD 69

FIGURE 5.17 REACTIVE POWER FOR ALL NOISE VARIANCES WITH AND WITHOUT VSG FOR FIREFLY ALGORITHM 70
FIGURE 5.18 REACTIVE POWER FOR ALL NOISE VARIANCES WITH AND WITHOUT VSG FOR ABC ALGORITHM 70

Chapter 6

FIGURE 6.1 MICROGRID COST STUDY PROJECT DATA BY NUMBER OF PROJECTS 75
FIGURE 6.2 COMMERCIAL MICROGRID HISTOGRAM 78
FIGURE 6.3 COMMUNITY MICROGRID HISTOGRAM 79
FIGURE 6.4 MILITARY MICROGRID HISTOGRAM 79
FIGURE 6.5 PCA FOR GENERATION CAPACITY 81
FIGURE 6.6 DATA DISTRIBUTION AFTER REFERENCE TRANSFORMATION 83
FIGURE 6.7 PCA AIMS TO GENERATION CATEGORIES 84
FIGURE 6.8 DATA DISTRIBUTION AFTER REFERENCE TRANSFORMATION 85

List of Tables

Chapter 3

TABLE 3.1 LIST OF PARAMETERS FOR GENERATORS. 29

Chapter 4

TABLE 4.1 LIST OF LCL STRUCTURE COMPONENTS. 41
TABLE 4.2 LIST OF PARAMETERS FOR GENERATORS. 49
TABLE 4.3 PARAMETER VALUES FOR PI CONTROLLER. 50-51
TABLE 4.4 D $_{1-0}$ % WITH AND WITHOUT VSG CASES 56

Chapter 5

TABLE 5.1 COMPARISON OF TIME TO REACH AVERAGE OPTIMAL INCREMENTAL COST FOR LAGRANGE AND PSO METHODS 61
TABLE 5.2 COMPARISON OF TIME TO REACH OPTIMAL LEVELS OF PARAMETERS FOR 0.8 NOISE VARIANCE 62
TABLE 5.3 DIFFERENCE OFFSET RATIO FOR LAGRANGE METHOD 72
TABLE 5.4 DIFFERENCE OFFSET RATIO FOR FIREFLY ALGORITHM 72
TABLE 5.5 DIFFERENCE OFFSET RATIO FOR ABC ALGORITHM 72

Chapter 6

TABLE 6.1 CONTRIBUTION OF THE VARIABLES (%) TOWARDS GENERATION CAPACITY 82
TABLE 6.2 CONTRIBUTION OF THE VARIABLES (%) THAT AIMS TO GENERATION CATEGORIES 85

Chapter 1. Introduction

Energy is an important aspect for the economic development of a country. Energy is important for overall development and is considered as the main infrastructural requirements for agricultural, industrial and socio-economic development and also for employment generation in rural and remote areas. With the increasing world population and the rising living standards, the global energy demand is steadily increasing. The demand for energy is predicted to increase by 60% by 2050, with the developing countries accounting for two-thirds of this increase. Energy security, as an issue of national strategic importance, has taken the center stage of the planning process against the backdrop of frequent rise in global crude oil prices. Energy security is essential to achieve national economic development goals and improve the quality of life of people. The level of per capita energy consumption has for long been considered as one of the key indicators of economic growth. The continued dependence of the nation on fossil fuel is loaded against it with inherent price volatility linked to finite global reserves. In addition, global warming, caused largely by greenhouse gas emissions from fossil fuel generating systems, is also a major concern. Thus, it becomes inevitable to use the renewable sources of energy along with conventional sources to meet the growing demand of energy. To reduce the CO_2 emissions from the combustion of fossil fuels, the use of renewable energy resources is necessary. Due to high penetration of Distributed generators (DGs) in distribution networks, grid-connected and islanded mode of operation is crucial for our energy requirements. Efficient development of microgrids will help more reliable power delivery, reduction in power losses and better frequency and voltage profile of the system. Stable and efficient operation of microgrids require new control, protection and communication infrastructure developments. Hence, microgrids stability must be achieved by subjecting novel control methods. Since the past couple of years, a significant amount of research has been carried out and funded in study microgrids.

Microgrids (MGs) are a combination of DGs, energy storage and loads. Their advantage is that they can be operated in grid connected or islanded mode. An efficient control strategy is needed in order to control the microgrids’ voltage and frequency and is crucial for its stable and reliable operation. These control strategies are also known as ‘Microgrid controller’. Intensive research has been carried out by professionals for an effective microgrid control using multiple algorithms and proposal of new approaches.

These control systems can be centralized, distributed or decentralized depending on the application, location, and economic viability of microgrid projects. Communication between these various control systems ad DGs is also important for a seamless operation of microgrid. It is also important to ensure that there are fewer communication gaps due to system lag or noise. This dissertation focuses on study of consensus-based approach for reduction in communication noise and simulation is carried to analyze its impact on overall power quality and cost of the microgrid system. Lagrange method and Particle swarm optimization (PSO) algorithm are compared to observe their active power performance and optimal dispatch solutions in grid-connected microgrids.

Also, reactive power compensation is performed in isolated microgrids for better active power and reactive power control of the system. Virtual synchronous generator is also assessed in conjunction with consensus-based approach to understand how these two methods provide for a more stable microgrid ecosystem. Lagrange formulation and Particle swarm optimization technique are compared to analyze their effect on grid-connected microgrid’s overall performance with and without VSG control approach. The Lagrange method, Firefly, and Artificial bee colony algorithm are compared for their voltage, output power, power factor, phase angle, and optimal dispatch performance in presence and absence of VSG-STATCOM strategy for various noise levels.

Chapter 2. Literature Review

2.1 Existing Methods

Economic dispatch is important for operation of microgrids. It helps in reducing the total cost of operation and generation of microgrids while meeting all the defined constraints. Since microgrids consist of distributed generators, it is imperative for these generators to communicate seamlessly with each other. This should be done with minimum losses and ensuring stable operation of the microgrid. Economic Dispatch is an optimization problem, which is used to minimize the cost of the system. It is one of the important problems in the field of power systems. While finding minimum cost of the system, all the constraints (both equality constraints and inequality constraints) of the system are taken into consideration. Many methods have been used to solve economic dispatch problem, most commonly by quadratic convex function [1], [2]. In [3] and [4] Lagrangian relaxation technique and quadratic programming has been used respectively. Particle Swarm Optimization has been used in [5] for effective demand response in islanded microgrids. [6] and [7] have used the Dragonfly algorithm and Cuckoo Search Algorithm to solve demand response in economic dispatch problems respectively. [8] introduces an improved Genetic Algorithm for optimal dispatch. Programming approaches for mathematically based optimization, such as Lambda-iteration, Gradient, Newton method, Base-point participation factor method, and others, can be used to resolve economic dispatch [9]. Many researchers have chosen to use artificial intelligenceand optimization techniques to solve Economic Dispatch. This contains hybrid techniques, which improve one technique's performance while using another to discover a superior answer. To address ED, it has been recommended that the Genetic Algorithm (GA), Particle Swarm Optimization (PSO), Differential Evolution (DE), Firefly algorithm, etc., be utilized [10]-[14].

Consensus based algorithms have been studied widely by ensuring the equal increment cost criterion [15]-[18]. To minimize the total cost, both economic dispatch and demand side management problems were solved [19]-[25]. The conventional economic dispatch problem assumes that the system/microgrids are noiseless. In real-time, noises are present in the system (from components as well as surroundings). This affects the performance and resilience of the microgrids. It also limits their stability. Hence, it is necessary to include noise in consensus-based algorithm economic dispatch problem, to stabilize the microgrids and enhance their resiliency and performance. Some publications have included noise in their analysis [26]-[28]. They developed noiseless control algorithm for voltage and frequency synchronization in microgrids as well as power sharing approach which is independent of its parameters. But not much research has been carried out in this area and therefore, this paper will explore towards this approach. [29] has discussed this strategy for islanded microgrids but did not include grid connected microgrids. This paper represents the noiseless economic dispatch problem for grid-connected microgrids. Also, in this approach there is no need of central controller, hence the system is more cyber secure and less expensive. Since a distributed approach is utilized, it eliminates the need of central controller and reduces communication complexity [30]-[35].

Inverter has a principal role in the interactive process of the microgrid and distribution network [36]. Droop control strategy [37] is used conventionally but it is very sensitive to fluctuations in load. Many literatures have proposed an improved droop control strategy based on the output voltage of inverter, but the frequency is not stable enough because of droop coefficient. An adaptive droop control strategy based on discrete consensus has also been proposed in DC microgrids [38-39]. P/Q control strategy has been used in grid-connected mode. U/f control strategy has been used predominantly in islanded mode. P/Q and U/f control strategy may be used together to form a new strategy. However, it is complicated as one needs to design two sets of control systems as well as switching control part for the two strategies [40]. FACTS devices have been predominantly used to provide compensation for voltage and phase angle instability [41]. This instability in the system could be due to load fluctuations or inherent noise in the system. STATCOMs are one of the commonly used devices for this purpose amongst many others. This paper uses STATCOM based controller to provide voltage and phase angle stability to the islanded microgrid during different noise conditions in a short span of time. STATCOM uses voltage source converter to provide shunt compensation in the microgrid system [42]. Another advantage is that it provides less damping, low harmonics, better response and improved voltage profile in the system [43].

2.1.1 Importance of Grid-connected Microgrids

Microgrid can operate in two modes: grid-connected mode and islanded mode. For majority cases, the microgrid and main grid are connected and communicate and operate both ways. If the main grid system fails or becomes inoperative, the microgrid is expected to operate independently. Hence, the microgrid should be able to disconnect from the main grid and operate in islanded mode. While connecting disconnecting from main grid and with inclusion of multiple generation sources, it is important to have good communication and control between all the components of microgrid. Many control strategies have been proposed to make micrograms more resilient and reliable. This chapter covers some of these strategies though literature survey.

A strategy to control the harmonic current of the voltage source grid-connected inverter according to the superposition principle, is proposed in [44]; PQ control, V/F control, Droop control and many more methods have ben discussed and proposed thoroughly in many literatures. [45] proposes hierarchical control, which uses layered-based algorithm to achieve control of microgrid. By adding idle mode between charging mode and discharging mode of energy storage system, [46] proposes control in the storage aspect of microgrids. [47] proposes that a system that uses current amplitude control method for inverter control during LVRT. This helps in avoiding the generation of output overcurrent. It also proposes that if the DC-DC converter abandons the maximum power tracking control when the grid side voltage drops, the fluctuations in voltage are more stabilized. [48] adopts the master-slave control mode. It helps control the “multi-micro source low-voltage” microgrid. It was observed that this method improves the power supply reliability in the microgrid. In this paper, the method of grid-connected PQ control and islanded droop control is introduced. It observes the microgrid system under different operating conditions. This control method is simple and warrants the utilization rate of the system. It also makes the switching process between different elements much easier and seamless [49].

As AC power system is more customary, a lot of investigations have been done in AC microgrids. However, with increase in application in remote areas, the inclusion of DC distributed generation (DG) units, storage elements (SE) and DC loads, DC microgrids have gained much popularity recently [50]. Islanded DC microgrids use a hierarchical control strategy based on droop control is proposed to achieve power management [51]. In [52], a two level control architecture based on bus-signaling and virtual inertia is proposed in an islanded DC Microgrid. This helps in achieving a more coordinated control strategy between various renewable energy sources/generation sources, local DC loads, and energy storage systems. In [53], many control strategies for DC microgrids have been studied and explored. Most of the research work is on the islanded mode of operation. It doesn’t address any coordinated operation of DC microgrids grid- connected mode.

[54]-[55] introduce different power management techniques based on dc bus voltage for integrated isolated DC microgrids. This technique is only for nonrenewable sources. However, it was observed that oscillations in bus voltage can cause switching of sources, which is not economical and reliable for nonrenewable sources. [56]–[57] tried to compensate for the above-mentioned issues. They did so by creating a centralized

controlling for various sources and loads. They also incorporated supercapacitor (SC) for smooth mode transitions, which also helps in increasing battery's life. [58] proposed an energy management approach that relies on battery's state of charge (SoC). However, it does not achieve full utilization of the battery due to its cutoff limits (i.e., 50% of SoC) and DG is operated in not so optimized fuel-efficient range. Authors in [59] developed a polynomial controller for all the source converters. However, it does not include fuel-efficient operation. This is because a DG is supplied variable power continuously to maintain the voltage of dc bus. The strategy proposed in [60] utilizes continuous operation of a DG for dc bus voltage regulation, which is not reliable and also leads to uneven loading.

In all the above-mentioned cases, power is converted into dc. In many applications, such as data centers, some loads must be fed through ac power. Hence, an ac bus needs to be formed. This can be done by an interfacing converter to supply the ac loads. [61] explains about the ac bus coupled isolated DC microgrids where a DG is connected on its ac power side. It proposes a solution by considering the SC to avoid startup delay of the DG and smoothens the dc bus voltage regulation. It does not consider a base station as dc load that increases the conversion losses, and does not explore the energy management scheme under all conditions. [62]-[63] propose an effective control and energy management techniques for grid-connected DC microgrids. They are not appealing since continuous operation of a DG is not economical and efficient. [64]-[65] introduce control and management strategies for integrated isolated DC microgrids. But there is no back-up source and hence may not be very suitable. Power management techniques are introduced in [66] for hybrid ac–dc microgrids. They use multiple sources on ac side. It also includes utilities where one source forms the ac bus and other source injects power based on the reference bus.

2.1.2 Importance of Islanded Microgrids

Usually, a Microgrid can operate while connected to a main grid network or medium voltage network. When a preplanned or unplanned event occurs in the main grid or medium voltage network, the Microgrid operates in isolated/islanded mode. If the microgrid switches to islanding mode because of fault or low voltage, the controllers must refrain the system from frequency and voltage fluctuations in order to send the quality power to consumers. The Microgrid should also be able to recover quickly from any frequency and voltage changes in islanding mode. When Microgrid switches to islanding mode, its previous condition should be analyzed. For example, if it was importing energy then after switching to islanding mode, it should be able to increase its generation capacity in order to compensate for the power lost. In another example, if it was exporting energy and it switches to islanding mode, it should be able to decrease its generation capacity so that the grid frequency can increase.

A considerable amount of research has been published on the control strategies of Microgrids. Reliable and quick control of real and reactive power are important for stability during transient and steady-state operation of a Microgrid [67]. For AC islanded microgrid, the output voltage of the system will fluctuate due to disturbances, such as the change in system parameters and power load. Research on controlling of inverter system of an islanded microgrid with strong robustness high reliability has an important implications its operation. To address deviation in voltages, the research on a microgrid inverter system includes the following methods: artificial intelligence control algorithm, robust control method, nonlinear control method, and disturbance observer (DO)-based control method. In [68], the particle swarm optimization algorithm is adopted to establish a grid-connected inverter system model. It also includes nonlinear links and harmonic disturbance of the power grid to achieve anti-interference control. [69] discusses method using a fuzzy neural network to achieve online compensation of external uncertainties caused by DC voltage fluctuation of inverter system. For an unexpected shutdown of the distributed power supply, the non-convex condition in the optimization problem was transformed into a convex linear matrix inequality condition in [70]. This method was able to adjust power sharing between the system load voltage and the distributed power supply. However, these methods are difficult to analyze system stability as they are not analytic. In [71], the optimal transient performance of H2 control and the anti-interference performance of $H\infty$ control are integrated. It introduces a mixed optimal control method of $H2/H\infty$ to account for parameters variations. This process is very complicated and not easy to perform. In [72], the Bialternate matrix is used to analyze the stability domain of the hybrid microgrid system. Using uncertainty in parameters of distributed power supply with inverter, it designs the parameters of a power stabilizer to ensure that the microgrid system has more stability.

[73] uses the unconstrained vector of the continuous control set to predict the change of load current in systems. It helps enhance the anti-disturbance performance of the inverter system with change of external load. The model predictive control (MPC)

voltage controller is combined with discrete time sliding mode control (SMC) current controller in [74] to improve the recovery ability of voltage and current. It considers load change, transient short circuit, and unbalanced phase in its analysis. In [75], SMC strategy is used to predict the harmonic current disturbance. It also filters the parameter perturbation generated by a nonlinear load in the microgrid system in real time. It helps in achieiving global robust control. According to [76], recursive terminal sliding mode control strategy is able to resist load variation for a distributed low-voltage microgrid either in grid-connection mode or islanded mode. However its disadvantage is that the redundancy of the MPC method information is quite high. This increases the complexity of the algorithm. [77] addresses the harmonic distortion due to nonlinear loads and background harmonics. The paper also proposes harmonic impedance reinforcement based control for voltage controlled DG inverters. In [78], a unified inertia index is introduced to evaluate the holistic inertia level of the hybrid microgrid. This method improves stability and dynamic performance of hybrid microgrid. In [79], a Kalman estimator-based voltage prediction control method is proposed for the interference of line impedance parameter change, load change, output impedance change, and distributed power supply fault. It helps in realizing the voltage free deviation control of an AC island microgrid without communication. In [80] active disturbance rejection control method is introduced which is based on the linear extended state observer (ESO) and is adopted to enhance robust control of the output current of a grid-connected inverter system.

In [81] peak load carrying capability (PLCC) of a distribution system is acquired from Loss of Load Expectation (LOLE) risk level. The proposed method employs microgrid unavailability criterion, and evaluates PLCC of a practical resilient microgrid in the islanded mode of operation. However, no solution is provided in the paper on how to calculate PLCC of an islanded microgrid for a specific reliability criterion.

2.1.3 Existing Microgrid Control & Management methods

Master-slave control is a typical control method of microgrids and discussed in many research articles. It has a master converter which acts as a grid-interface converter under grid connection mode and acts as an energy storage converter under island mode. It works in voltage source mode to control DC bus voltage. The rest work as slave converters that employ current source to participate in the power management of the system. This method has many advantages, to name a few— (1) it has a simple control structure, (2) quick response for power management and (3) robust bus voltage dynamic performance. However, during fault seamless transmission performance depends on communication and master converter [82]-[83]. Also, its reliability and scalability are very less. Peer-to peer control is another method for microgrid control to improve reliability and scalability [83]. In this method, the upstream grid and energy storage unit with voltage support function in the system operate in a drop mode. The system power balance and stability of the DC bus voltage is achieved by detecting the DC bus voltage signal. This is done using their own drooping curve. This helps in increasing the reliability of the system and the plug-and play function can also be used. However its disadvantage is that it has slower response to power management and also needs another secondary level control to improve performance of DC bus voltage. Many researchers have proposed an improved method based on secondary control [84]. These methods have also increased the complexity of microgrid control.

In [85], an improved master-slave control strategy based on I-ΔV droop is proposed. It also combines the advantages of peer-to-peer control and controls seamless transition between grid-connected mode and islanded mode. It helps energy storage unit to operate under current control like conventional master-slave control during grid connection. It provides for a seamless transition to voltage control based on I-ΔV droop during islanded mode of operation.

In [86]-[87], the communication network plays a critical role in smart microgrids. This is because of increment in number of renewable resources and microgeneration units that are being connected to microgrids. Due to this increase in number of elements of microgrid, the communication must be able to handle an increasing amount of data traffic or services requests. It should also be able to provide real-time monitoring and control operation of all the elements, and hence preferably switching from a centralized to a decentralized communication [88]. Successful evolution and penetration of smart microgrids requires the development of distributed communication architectures and protocols [89]-[90]. In [91]-[92] Multi-Agent Systems technology has been introduced for power system management. In this type of technology, each DER unit is considered as an agent. An agent is defined as a computer system that is able to perform tasks in an autonomous way and has capabilities to communicate with their neighbor agents. These agents solve problems through cooperation, coordination and negotiation. These agents have a drawback of not having ability to reorganize themselves. This drawback may result in a lack of knowledge about the global status of the microgrid. It may also lead to sub-optimal resources allocation and poor management of resources and hence a less stable microgram ecosystem [93]. To overcome these limits, recent researches [94-97] use Peer-to-Peer (P2P) communication networks for microgrid environments. In these cases high efficiency, quality network requirements and flexibility is needed [98-100]. Peer-to-peer networks are developed for file and processor cycle sharing, and their network performance requirements are less critical [101]. Therefore, the need is to develop a protocol that is able to adapt to network quality performance requirements of Smart Microgrids. However, performance of the communications network layer is not extensively covered by research papers, although it is an important component for new Smart Microgrids. In this paper [102] a new decentralized communication infrastructure and a new protocol for microgrid monitoring and control is proposed. All the agents interact over Peer-to-Peer (P2P) overlay network for a better and smarter microgrid.

2.2 Research Motivation

From the reviewed literature, some limitations were observed in microgrid control technology. At first, most papers consider the microgrid system to be noise free. However, this is not true in real-time applications. Lots of fluctuations and malfunctions occur due to noise from different microgrid networks, its environment and location. Also, communication between different agents also has some amount of noise interference which affects overall power, frequency and voltage quality. To overcome this shortcoming, consensus based approach has been analyzed for grid-connected mode. For islanded mode, consensus based approach has been analyzed with reactive power compensation using STATCOM controller. Also, droop control and VSG control strategy have been studied and compared in various literatures. However, including noise with VSG technology has not been researched thoroughly. This dissertation makes an effort in analyzing this segment of microgrids for a stable and more resilient system. It does so by comparing 4 different algorithms. For active power, Lagrange method and PSO algorithm have been compared for grid-connected microgrid. For reactive power compensation and in isolated mode, Lagrange method, Firefly algorithm, and Artificial Bee Colony algorithm have been compared.

Chapter 3. Economic Dispatch and Consensus based algorithm

3.1 Problem Formulation for Economic Dispatch

Economic Dispatch is an optimization problem used to minimize the cost of the system. It is one of the important problem in the field of power systems. While finding minimum cost of the system, all the constraints (both equality constraints and inequality constraints) of the system are taken into consideration. Many methods have been used to solve economic dispatch problem, most commonly by quadratic convex function [1], [2]. In [3] and [4] Lagrangian relaxation technique and quadratic programming has been used respectively. Consensus based algorithms have been studied widely by ensuring the equal increment cost criterion [5]-[8]. To minimize the total cost, both economic dispatch and demand side management problems were solved [9]-[15]. For future work, mixed integer programming will be analyzed to solve economic dispatch problem. The conventional economic dispatch problem assumes that the system/microgrids are noiseless.

3.1.1 Lagrange method

The Lagrange method is used to define the economic dispatch problem for grid-connected microgrid. First, the objective function of the microgrid is defined. This function is most commonly used in solving economic dispatch problems. Considering i (1, 2, 3,…, n) units of generation in a microgrid system, the cost of a generator can be defined in terms of a quadratic equation. The units' cost function is described in the quadratic equation (1a). P_{loss} has been assumed as 7% of the total load.

$$\sum_{i=1}^{n} C_i P_i = \sum_{i=1}^{n} a_i P_i^2 + b_i P_i + c_i \tag{1a}$$

For economic dispatch problem, we want to minimize the generation cost of the microgrid. Equation (1a) becomes:

$$\min \sum_{i=1}^{n} C_i P_i = min \sum_{i=1}^{n} a_i P_i^2 + b_i P_i + c_i \tag{1b}$$

Also, total power output of generator can be defined as:

$$\sum_{i=1}^{n} P_i = P_D + P_{loss} \text{ , for } P_i^{min} < P_i < P_i^{max} \tag{1c}$$

Where, P_D is the total load and P_{loss} are the losses incurred during transmission of power from generation units to the loads. P_i^{min} is the minimum generation limit of generator i and P_i^{max} is the maximum generation limit of generator i.

To formulate the Lagrangian function, equation (1a), (1b) and (1c) becomes:

$$L(P_1, P_2, \ldots P_n) = \sum_{i=1}^{n} C_i P_i + \lambda\left(P_D + P_{loss} - \sum_{i=1}^{n} P_i\right) + \sum_{i=1}^{n} u_x\left(P_i - P_i^{max}\right) + \sum_{i=1}^{n} u_y\left(P_i^{min} - P_i\right) \tag{2}$$

To find a solution of the above economic dispatch problem, incremental cost (IC_1, IC_2,…, IC_n) for each generator should be calculated. To find the minimized cost of the microgrid, these incremental cost for different generators should be equal to each other, i.e.,

$IC_1 = IC_2 = \ldots = IC_n$

Solution to this problem, is most commonly used solution:

$$\lambda_i = \frac{\partial C_i P_i}{\partial P_i} = 2a_i P_i + b_i = \lambda^* \qquad P_i^{min} < P_i < P_i^{max}$$

$$\lambda_i = \frac{\partial C_i P_i}{\partial P_i} = 2a_i P_i + b_i < \lambda^* \qquad P_i = P_i^{max}$$

$$\lambda_i = \frac{\partial C_i P_i}{\partial P_i} = 2a_i P_i + b_i > \lambda^* \qquad P_i = P_i^{min} \tag{3}$$

So, the economic dispatch problem has to take into account generation limits for each generator to find an economic dispatch schedule for the microgrid. If there are no equality or inequality constraints to be considered for the generators, then it is fairly easy to solve economic dispatch problem. However, most of the problems have some constraints that need to be considered while solving economic dispatch problem for microgrids. The above equations provided are the basic problem formulation for any economic dispatch related problems and have been used for this dissertation's calculations as well.

3.1.2 Particle Swarm Optimization (PSO) algorithm

Particle Swarm Optimization is a computational method that was inspired by the movement of bird flocks and other organisms/particles by Kennedy, Eberhart, and Shi [144]. It is a population-based optimization tool in which particles change position by taking into account their velocity, their own experience, and the experience of their neighboring particles. The position and velocity of particle *j* in N-dimensional space are represented as $a_j = (a_{j1}, a_{j2}, \ldots a_{jN})$ *and* $b_i = (b_{j1}, b_{j2}, \ldots b_{jN})$. The best position for this particle can be represented as $Abest_j = (a_{j1}^A, a_{j2}^A, \ldots\ a_{jN}^A)$. Best position for the neighboring particle can be represented as $Bbest = (a_1^B, a_2^B, \dots a_N^B)$. New modified position and velocity can be formulated as:

$$b_{jN}^{k+1} = \xi .\, b_{jN}^{k} + m_1 r_1 *(Abest_{jN} - a_{jN}^{k}) + m_2 r_2 *(Bbest_N - a_{jN}^{k})$$

$$\text{and, } a_{jN}^{k+1} = a_{jN}^{k} + b_{jN}^{k+1} \tag{4}$$

Where

k	number of iterations
ξ	inertia weight factor
m_1, m_2	acceleration constant
r_1, r_2	Random number within range [0,1]

Inertia weight factor and acceleration constant affect the performance abundantly. The weight factor provides the required momentum for particles to move around in N-dimensional space. The acceleration constant signifies the weight of stochastic acceleration terms that help in pulling all particles towards $Abest_j$ and *Bbest* positions. This algorithm is used iteratively to find convergence in optimal dispatch solutions. The best incremental cost is determined using this method which is then sent to the agents to either accept or modify the output power of generators to minimize the effect of noise on system parameters' fluctuations.

3.1.3 Firefly algorithm (FA)

To solve holistic optimization problems, Xin-She Yang [145] developed the Firefly Algorithm. FA was created in response to firefly flashing activity. The algorithm introduces the following three ideal rules [145]: One firefly is drawn to another firefly regardless of its gender because: 1) all fireflies are considered unisex; 2) attractiveness is inversely correlated to light brightness; thus, for any two fireflies that are flashing, the less bright one will always move toward the more bright fly; and 3) a firefly's brightness is dependent on the outlook of the objective function. The brightness for maximizing problems can simply be proportional to the objective or fitness function's value. Two principles of the firefly algorithm are: (1) The variation in light intensity; (2) How attraction is established/formulated. We are free to presume that a firefly's attraction is influenced by its brightness. Fig. 3.1 flowchart showcases incorporation of Firefly Algorithm for economic dispatch problem.

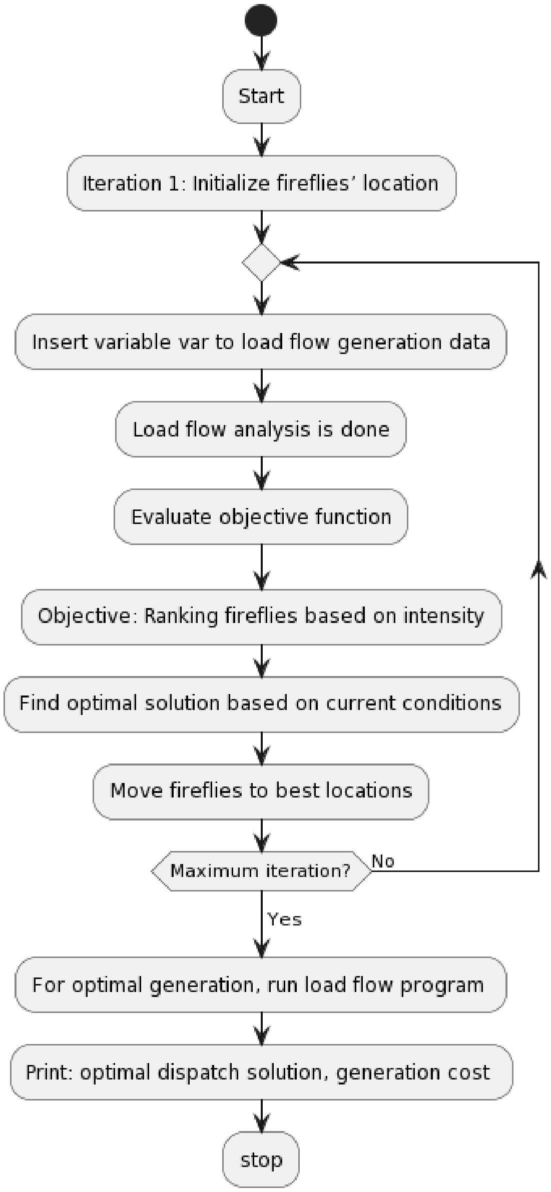
Start
Iteration 1: Initialize fireflies' location
Insert variable var to load flow generation data
Load flow analysis is done
Evaluate objective function
Objective: Ranking fireflies based on intensity
Find optimal solution based on current conditions
Move fireflies to best locations
Maximum iteration?
No
Yes
For optimal generation, run load flow program
Print: optimal dispatch solution, generation cost
stop

Fig. 3.1 Flowchart for ED solution using FA

3.1.4 Artificial Bee Colony (ABC) algorithm

Artificial Bee Colony (ABC) method is an optimization technique that replicates honey bee foraging behavior. It has been effectively used to solve several real-world issues. Developed by Karaboga in 2005 [146], ABC is a member of the class of swarm intelligence algorithms.

A group of honey bees known as a swarm can work together to complete tasks successfully. There are three different kinds of bees considered in this algorithm: employed bees, observer bees, and scout bees [146]. The employed bees look for food nearby the food source in their memories while also informing the observer bees about the food sources. The observer bees' job is to select the food source with greater quality i.e. fitness. The scout bees have originated from a few employed bees. These are those employed bees that leave their food sources and look for new ones. The employed bees make up the first half of the swarm in the ABC algorithm, and the onlooker bees make up the other half.

The number of solutions in the swarm is equal to the number of employed or onlooker bees. The ABC algorithm creates an initial population of S_N solutions (food sources). These are spread randomly. S_N stands for swarm number. ABC algorithms' steps are described as follows [146]:

Step 1: Initialization Step. It generates a solution for a distributed population of a source of food. It is randomly generated and represented by swarm size. The following equation is the i^{th} solution for a swarm for dimension size of n.

$$S_i = \{S_1, S_2, S_3, \ldots, Sn\} \text{ ; n = dimension size.} \tag{5}$$

Step 2: Employed bee stage. Every employed bee visits a food source during the employed bee phase and creates a neighboring food source close to the chosen food source. Employed bees conduct a search (around each food source) to find a new solution.

$$X_{ik} = S_{ik} + u(S_{ik} - S_{jk}) \tag{6}$$

Where X_j = candidate solution selected randomly,

k = random dimension index Є (1,2, …, n),

u = random number Є [-1, 1].

Step 3: Onlooker bee stage. It is based on a probability value. The food source is chosen by the onlooker bee. The following formula is used to determine the likelihood that onlooker bees would choose a food source:

$$p_i = \frac{fitness_i}{\sum_{i=1}^{F_p} fitness_i} \tag{7}$$

Where p_i = probability for food source selection,

F_p = total food-source positions,

$fitness_i$ = fitness value for solution i.

Step 4: Scout bee stage. In case of step 2 and step 3 bee phases, if a food supply is not improved for a defined number of trials, the employed bee linked with that food source changes to scout bee status. The scout bee is then used to discover a fresh food supply.

3.2 Consensus-based Economic Dispatch for noiseless communication

In this section, the approach introduced in [28] is explained. The communication link for the microgrid is defined. There is an agent corresponding to each generator unit, which collects information from their respective units. This information is processed by a specific agent. All the agents in the communication system are also connected to each other. Since, our grid-connected mode microgrid has 4 generation units, we have 4 agents in total, and each connected to their specified unit. The information collected and processed by the agents is exchanged between each other. This exchange helps provide information regarding the present status of each unit. This information is used to change the output power from each unit (while keeping their constraints in check), to minimize the total cost of the microgrid system. Noise from the components, surroundings, electric/magnetic interference is some of the reasons assumed in this analysis. Noise accumulated due to communication between units as well as between units and agents has been included in this approach. They have been modeled as Gaussian noise [103]. Communication links can be selected as c_{12}, $c_{21,}$ $c_{23,}$ $c_{32,}$ $c_{34,}$ $c_{43.}$ Blackouts or incorrect departures from optimal economic dispatch might come from additive noise corrupting the communication lines between DGs. The consensus-based ED solution incorporates the post-iterate averaging technique specifically to handle these circumstances.

When the error norm converges to 0.05, the Monte-Carlo simulation comes to an end. IT confirms the effectiveness of this proposed algorithm. The noise variance values have been taken by authors' choice and should always have a value greater than 0.

Corresponding incremental cost of each unit is calculated by their respective agent and then exchanged with each other. Set point of output power is calculated based on the information and is sent to their respective generation units. Accordingly, the units change their power generation to have equal incremental cost to solve the economic dispatch problem. This leads to overall minimization of microgrid cost.

[28] has formulated this approach as follows:

$X[k+1] = X[k] + \mu[k][M\, x[k] + WD[k]]$

M = -H´GH

W = H´G

H = H_2-H_1 (8)

$$H_1 = \begin{vmatrix} 0 & 1 & 0 & 0 \\ 1 & 0 & 0 & 0 \\ 0 & 0 & 1 & 0 \\ 0 & 1 & 0 & 0 \\ 0 & 0 & 0 & 1 \\ 0 & 0 & 1 & 0 \end{vmatrix}$$

$$H_2 = \begin{vmatrix} 1 & 0 & 0 & 0 \\ 0 & 1 & 0 & 0 \\ 0 & 1 & 0 & 0 \\ 0 & 0 & 1 & 0 \\ 0 & 0 & 1 & 0 \\ 0 & 0 & 0 & 1 \end{vmatrix} ;\ H = \begin{vmatrix} 1 & -1 & 0 & 0 \\ -1 & 1 & 0 & 0 \\ 0 & 1 & -1 & 0 \\ 0 & -1 & 1 & 0 \\ 0 & 0 & 1 & -1 \\ 0 & 0 & -1 & 1 \end{vmatrix} = H_2 - H_1$$

G (small noise) = diag [0.2 0.2 0.2 0.2 0.2 0.2]

G (medium noise) = diag [0.5 0.5 0.5 0.5 0.5 0.5]

G (large noise) = diag [0.8 0.8 0.8 0.8 0.8 0.8]

For 3 generating units, the following matrices have been used for calculations:

$$H_1 = \begin{vmatrix} 0 & 1 & 0 \\ 1 & 0 & 1 \\ 0 & 1 & 0 \end{vmatrix}$$

$$H_2 = \begin{vmatrix} 1 & 0 & 0 \\ 0 & 1 & 0 \\ 0 & 0 & 1 \end{vmatrix} ;\ H = \begin{vmatrix} 1 & -1 & 0 \\ -1 & 1 & -1 \\ 0 & -1 & 1 \end{vmatrix} = H_2 - H_1$$

G (small noise) = diag [0.2 0.2 0.2]

G (medium noise) = diag [0.5 0.5 0.5]

G (large noise) = diag [0.8 0.8 0.8]

Similarly, M and W can be calculated using the formula given above.

Next step is to average the incremental costs of all the units in order to reduce the effects of noise. This will result in a more resilient and stable microgrid devoid of any (lesser) communication noise.

$$X_{avg}[k+1] = \frac{1}{k+1}\sum_{j=1}^{k+1} X[j]$$

$$= \frac{1}{k+1}\sum_{j=1}^{k} x[j] + X[k+1]$$

$$= X_{avg}[k] - \frac{1}{k+1} X_{avg}[k] + \frac{1}{k+1} X[k+1] \tag{9}$$

From (8) and (9), the noiseless economic dispatch approach is concluded as:

$$X[k+1] = X[k] + \mu[k][M\, x[k] + WD[k]]$$

$$X_{avg}[k+1] = X_{avg}[k] + \frac{1}{k+1}[X[k+1] - X_{avg}[k]] \tag{10}$$

The step size satisfies the following conditions: $\mu[k] \geq 0$, $\mu[k] \to 0$ as $k \to \infty$. The step size is taken as 0.67 using brute-force method. This method is iterative in nature and an estimate is made using the step size, which is then averaged in later stages to reduce the effect of noise. The consensus problem is solved iteratively for each step size. The flowchart for the consensus-based economic dispatch algorithm is shown in Fig. 3.2 below.

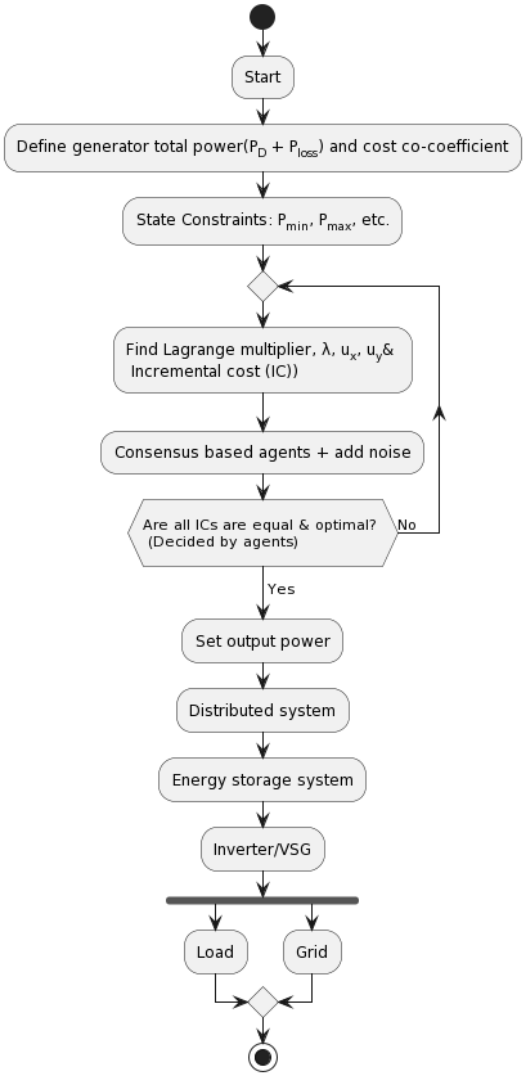
Start
Define generator total power($P_D + P_{loss}$) and cost co-coefficient
State Constraints: P_{min}, P_{max}, etc.
Find Lagrange multiplier, λ, u_x, u_y& Incremental cost (IC))
Consensus based agents + add noise
Are all ICs are equal & optimal? (Decided by agents)
No
Yes
Set output power
Distributed system
Energy storage system
Inverter/VSG
Load
Grid

Fig. 3.2 Algorithm Flowchart

3.3 Numerical Simulations

The grid-connected microgrid is analyzed under 4 different conditions. Initially the microgrid is studied when there is no noise in the system. The economic dispatch algorithm provided in the previous section is tested to see the performance of the system in absence of noise. In the second condition, noise of variance 0.2 is introduced in the system, and the performance is observed. During the third condition, noise variance is increased to 0.5 and for the final condition, the noise variance is set to 0.8. The performance of the microgrid under different noise conditions has been analyzed using MATLAB. The microgrid under analysis for this paper consists of 4 generator units. It is in grid-connected mode and has a solar/Photovoltaic (PV) generator, wind generator and 2 coal-based generator units. The units' cost function is described in the quadratic equation (1a). P_{loss} has been assumed as 7% of the total load. Cost-coefficients, minimum and maximum power generation limits of the units are provided in the table below. Although, P_{min} should be 0 for Unit 1 and Unit 2 (PV units), the values are non-zero to accommodate consistency of data procured. These minimum values do not affect the overall calculations for the system.

TABLE 3.1 List of parameters for generators

Unit	P_{min} (kW)	P_{max} (kW)	a	b	c
1	4	18	0.070	2.15	56
2	8	40	0.080	1.15	50
3	5	25	0.070	3.3	41
4	5	40	0.056	3.4	36

In all the cases, power output of the 4 generator units tries to maintain its optimal dispatch schedule with the introduction of different noise levels. In the end, a comparison has been made to show how the system stabilizes the incremental cost under various noise conditions.

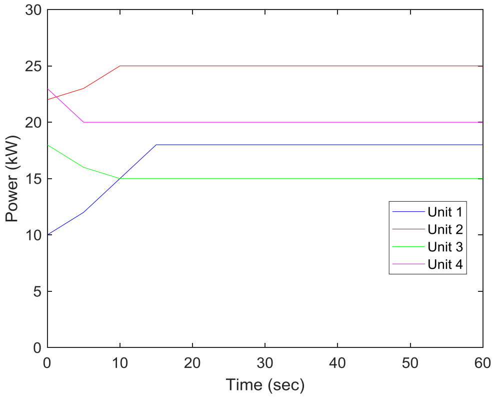

Fig. 3.3 Output power of generator units in kW without noise

Fig. 3.3 shows varying power output of the 4 generator units under 60 sec period. This case is simulated under noise free conditions. It takes around 15 sec for the system to reach a constant generating power output for high noise variance.

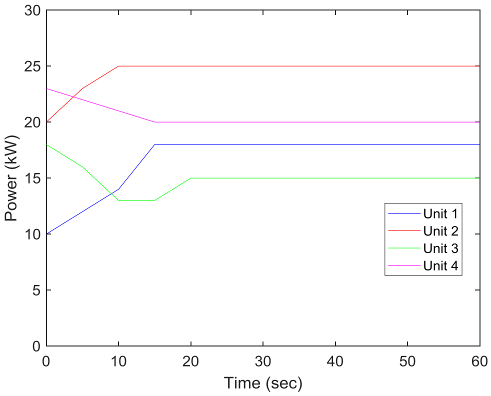

Fig. 3.4 Output power of generator units in kW with 0.2 noise variance

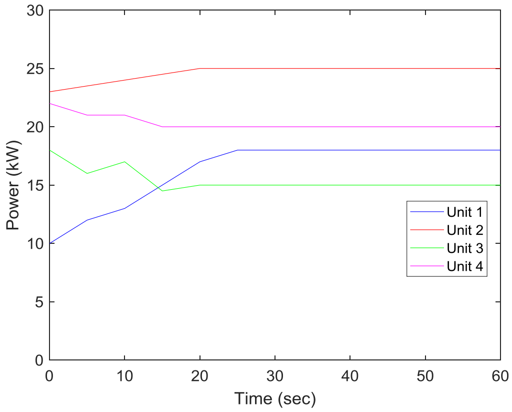

Fig. 3.5 Output power of generator units in kW with 0.5 noise variance

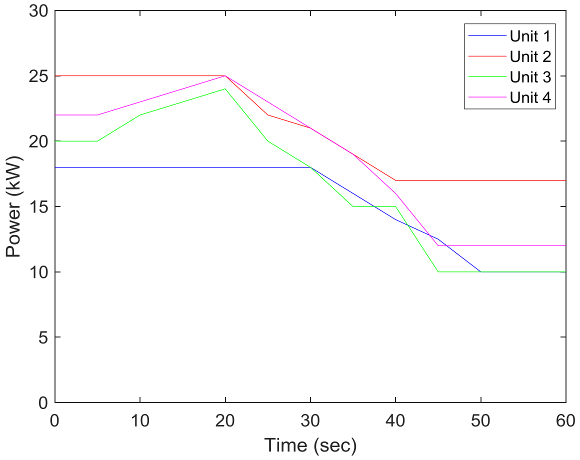

Fig. 3.6 Output power of generator units in kW with 0.8 noise variance

Fig. 3.4, 3.5 and 3.6 shows output during some noise variance. In this study, we have considered small (variance of 0.2), medium (variance of 0.5) and large (variance of 0.8) noise levels to simulate the system and observe its behavioral pattern for the chosen consensus-based algorithm. Due to less stability of the system for higher noise levels, the economic dispatch solution changes and is not as stable as observed for higher noise level of 0.8 variance. In all the figures below, it is visible that the system takes a couple of seconds to reach a constant value. As seen from the graphs, the output power reaches a constant value after sometime. For 0.8 noise variance, the output power takes a dip before reaching constant value. This dip is due to higher noise in the system which leads to more instability and provides a more undesired result.

The higher the noise, the more time it is taken by the system to reach to the desired value. For noise variance of 0.2, the system takes about 20 sec to reach its desired output. For 0.5 noise variance, it takes around 25 sec and 45 sec for 0.8 noise variance.

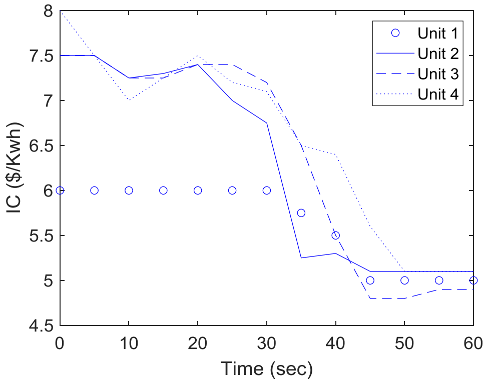

Fig. 3.7 Incremental Cost (IC) of generator units without noise

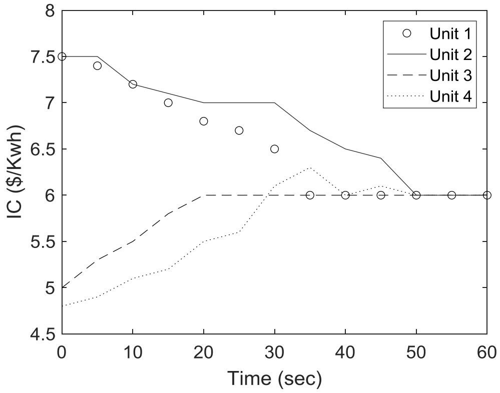

Fig. 3.8 Incremental Cost (IC) of generator units with 0.2 noise variance

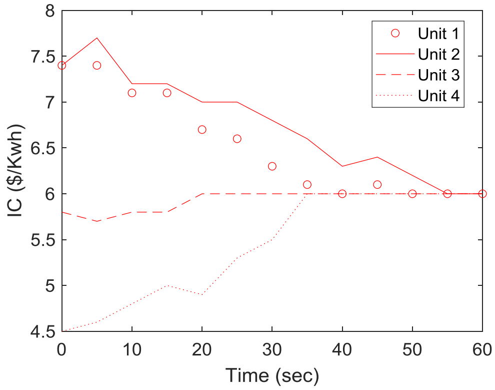

Fig. 3.9 Incremental Cost (IC) of generator units with 0.5 noise variance

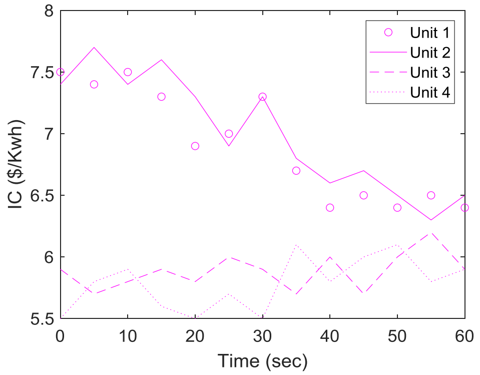

Fig. 3.10 Incremental Cost (IC) of generator units with 0.8 noise variance

Fig. (3.7), (3.8), (3.9) and (3.10) show incremental costs of the 4 generator units for no noise condition, noise variance of 0.2, 0.5, and 0.8 respectively. During no noise condition, the algorithm helps set the incremental cost of all the generator units at a faster pace. With increase in noise variance, it takes time to reach to consensus. For higher noise levels, as seen in Fig. 3.10, it was difficult to achieve consensus and the system still has some instability. But for smaller and medium noise levels, the algorithm worked effectively in weeding out noise in the system. The average incremental cost ($/kWh) comes out to be around 6 as seen from the graphs, which is close to the values calculated manually.

3.4 Discussions

This proposed algorithm was used to analyze the behavior of microgrid during grid-connected mode. The microgrid shows good response during less and medium noise level. It brings the system close to its set point for incremental cost in less time. However, it was observed that it took longer for the system to reach its set point for noise levels higher than 0.8 variance. The system oscillated around the set point value for a longer time and hence can be concluded that it was not stable to the desired level. Thus, this economic dispatch algorithm is very good for small and medium noises as it brings stability to the system in a short span of time based on the case study.

Chapter 4. Control Strategies

Since microgrids consist of distributed generators, it is imperative for these generators to communicate seamlessly with each other. This should be done with minimum losses and ensuring stable operation of the microgrid. With the use of distributed generators, instability is inherent in the system. In order to improve the power quality of the microgrid, a type of virtual synchronous generator (VSG) control strategy is introduced to control the microgrid with noiseless consensus based algorithm. The VSG model is based on stator voltage and rotor motion model demonstrated by deformation and vector decomposition of the hidden-pole synchronous generator second-order equation. It also introduces a STATCOM controller for reactive power management. The controller will help provide stability to the microgrid's voltage, output power and phase angle. This will enhance the microgrid's performance and make it a more resilient system. VSG strategy is also used with STATCOM to better under the reactive power fluctutations in the system.

4.1 Virtual Synchronous Generator (VSG)

The VSG control system [104] incorporates the VSG model, virtual frequency regulation module, virtual voltage regulation module, grid-connected control module, SPWM modulation module and sampling calculation module. It is responsible for simulating the system's performance and determining its optimal power output, the Frequency Regulation Module, which adjusts the frequency of the output power to match that of the grid, the Voltage Regulation Module, which regulates the voltage of the output power, the grid-connected mode of Control Module, which ensures the output power is synchronized with the grid, the SPWM Modulation Module, which adjusts the output current amplitude, and the Sampling Calculation Module, which calculates the output power by sampling the input signal. All of the modules work together, to provide a reliable and secure electricity management system as shown in Fig. 4.1.

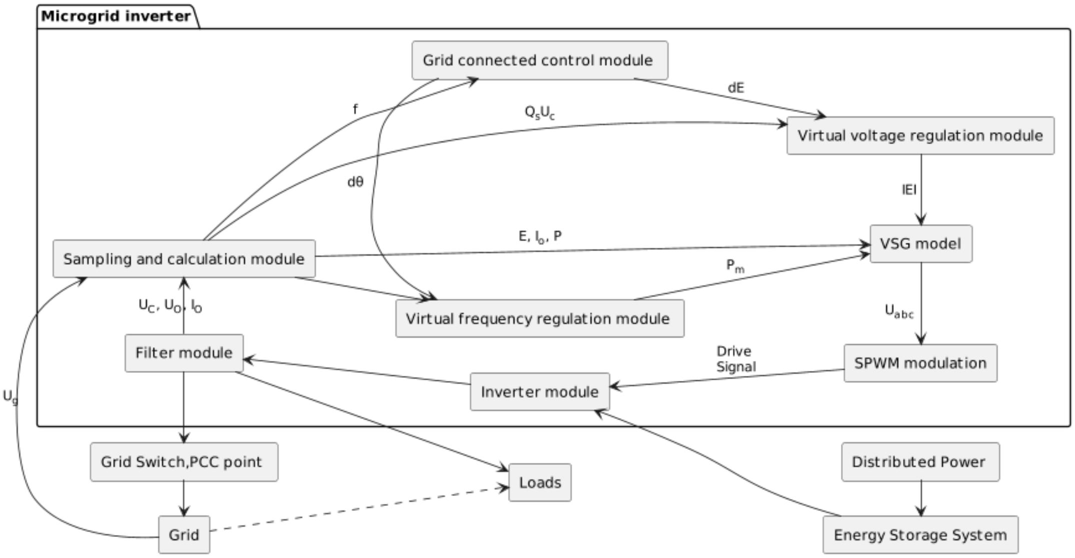
Microgrid inverter
Grid connected control module
dE
f
Q_sU_c
Virtual voltage regulation module
dθ
|E|
E, I_o, P
VSG model
Sampling and calculation module
P_m
U_C, U_O, I_O
Virtual frequency regulation module
U_{abc}
Filter module
Drive Signal
SPWM modulation
Inverter module
U_g
Grid Switch,PCC point
Loads
Distributed Power
Grid
Energy Storage System

Fig. 4.1 VSG control strategy block diagram

Traditional SG rotation has large moment of inertia and output inductance, and the control method is also mature. Therefore, by simulating the external characteristics of the microgrid into a SG, the microgrid powersupply is equivalent to the prime mover.

Electric energy generated by the distributed resources is supplied to the load through the inverter module and the filter module of the microgrid inverter, and the remaining electric energy is stored by the energy storage system.

The second-order equation modeling of the SG is presented in [96], which contains stator voltage equation and rotor motion equation. Stator voltage model is given in figure 4.2 below:

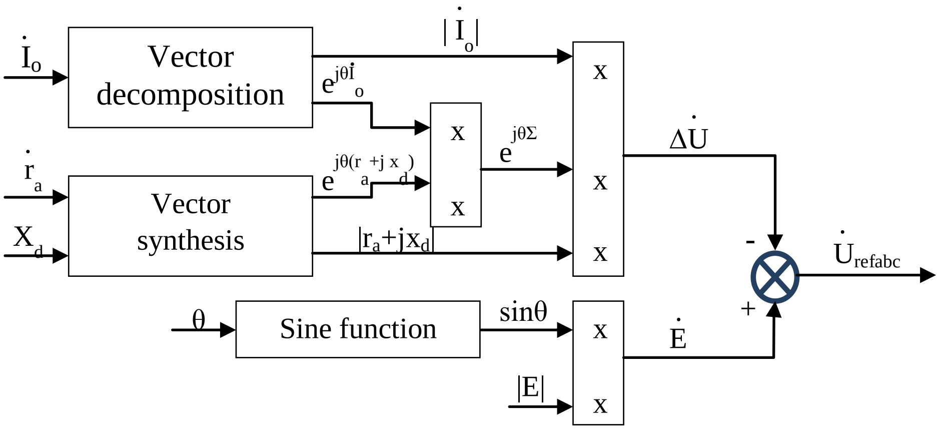

$\dot{I}_o$
Vector decomposition
$|\dot{I}_o|$
$e^{j\theta \dot{I}_o}$
$\dot{r}_a$
X_d
Vector synthesis
$e^{j\theta(r_a+jx_d)}$
$|r_a+jx_d|$
x
x
$e^{j\theta\Sigma}$
x
x
x
$\Delta\dot{U}$
-
+
$\dot{U}_{refabc}$
θ
Sine function
sinθ
x
x
$\dot{E}$
|E|

Fig.4.2 Stator voltage model

Stator voltage equation:

$$\dot{U}_{refabc} = \dot{E} - \Delta\dot{U} \tag{11}$$

The synchronous generator stator current is equivalent to output current I_0 of the inverter; r_a and X_d are VSG armature resistance and synchronous reactance respectively. For (r_a+jX_d) and I_O vector multiplication is performed to obtain ΔU. E is corrected by deviation to get U_{refabc}, and the subsequent SPWM modulation module generates a corresponding control signal in accordance with U_{refabc}.

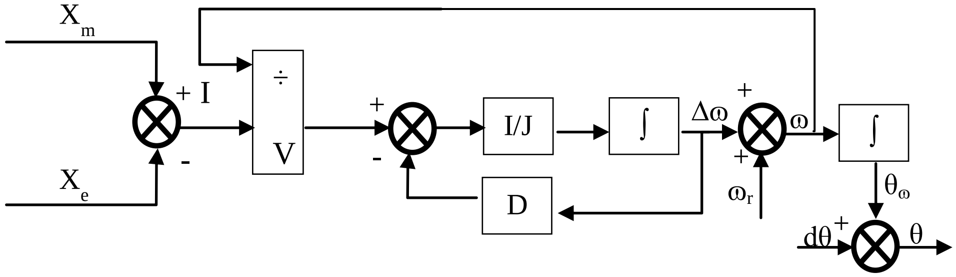

Fig.4.3 Rotor motion model

Fig. 4.3 shows that rotor motion model increases system stability. It does so by addition of *J* and *D* when P_m and P_e do not match. $d\theta$ is the correction angle of grid connection control module.

For the rotor motion model:

$$\Delta\omega = \frac{1}{J}\int\left(\frac{P_m - P_e}{\omega} - D\Delta\omega\right)dt \tag{12}$$

$$\omega = \Delta\omega + \omega_N \tag{13}$$

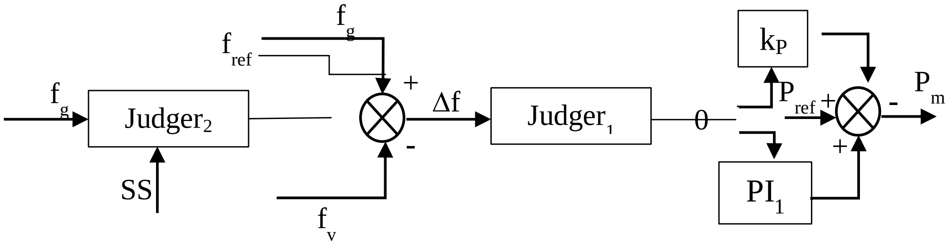

Fig. 4.4 Frequency regulation module

The frequency deviation, *Δf* is sent to Judger$_1$. Judger$_1$ decides whether to send it to the next stage regulator or ignore the difference according to the interval in which the difference is located. The frequency regulation module as shown in Fig. 4.4 controls the primary frequency regulation according to the VSG power-frequency coefficient kP, the secondary frequency regulation is simulated by PI_1. System frequency stability is maintained by the Synchronous Generator through primary frequency regulation and secondary frequency regulation. The secondary frequency regulation is realized in the frequency regulation unit. If the effect of the frequency regulation isn't sufficient, we can switch to the secondary frequency regulation.

The inputs to the voltage regulation module in Fig. 4.5 are reference reactive power Q_{ref} and VSG control output reactive power Q_o. The difference is multiplied by the voltage-reactive coefficient k_U to get reactive power adjustment electromotive force ΔE_1. The difference value between effective value of the capacitor voltage U_c in filter module and the reference voltage U_{ref} is converted into an amplitude to obtain the machine terminal voltage adjustment electromotive force ΔE_2. E_{ref} is the reference electromotive force when the VSG operates in no-load mode, dE is the corrected electromotive force of the grid-connected control.

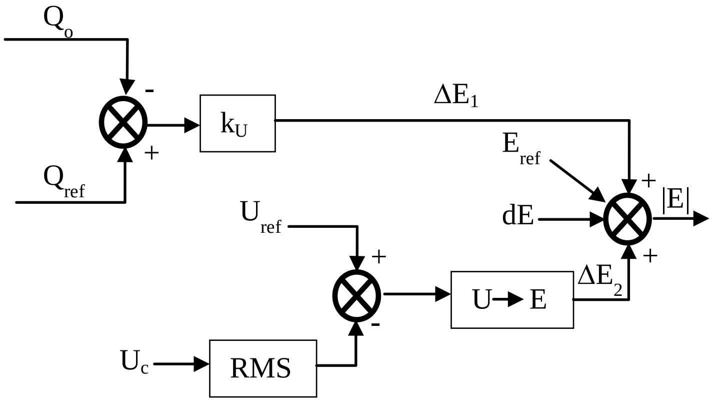

Fig. 4.5 Voltage regulation module

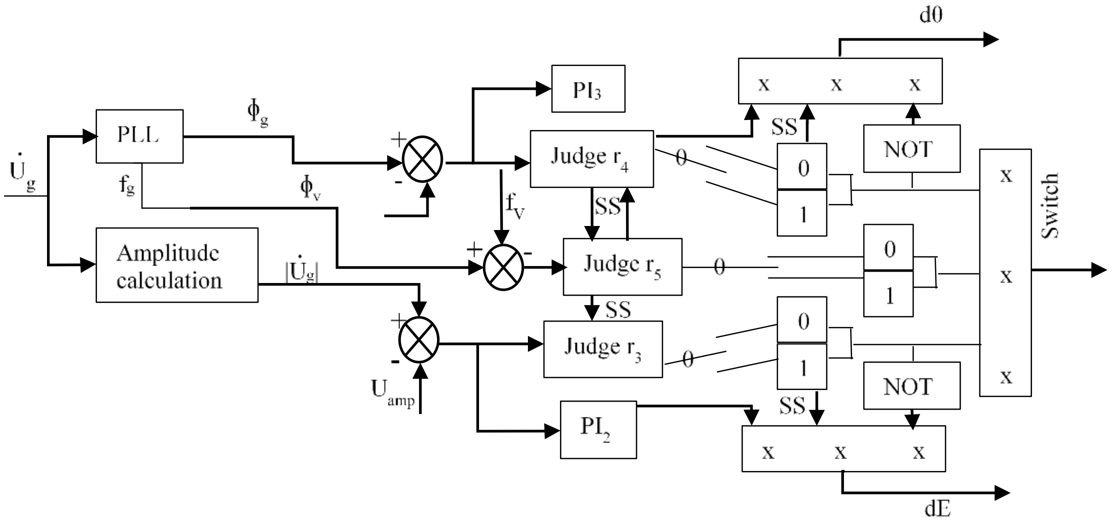
d0
x x x
PI3
SS
NOT
PLL
ϕ_g
$\dot{U}_g$
f_g
ϕ_v
+
-
Judge r_4
θ
0
1
x
Switch
f_V
SS
Amplitude calculation
$|\dot{U}_g|$
+
-
Judge r_5
θ
0
1
x
SS
+
-
Judge r_3
θ
0
1
NOT
x
U_{amp}
PI$_2$
SS
x x x
dE

Figure 4.6 Grid control module

The *U*-*Q* curve is as follows:

$$U - U_{SGref} = k_{SGU} (Q_{SGref} - Q) \tag{14}$$

The grid-connected control module with voltage phase angle dual feedback is shown in Fig. 4.6. When the step signal SS is changes from 0 to 1, pre-synchronization is performed by the grid-connected control module. The difference between voltage phase angles φ_g and φ_V is sent to the PI_3 regulator and $Judger_4$. The value sent by the PI3 is sent to the rotor motion model as *dθ*. $Judger_4$ decides the subsequent input value in accordance with the interval where the difference is located. The difference between $|U_g|$ and U_{amp} is sent to the PI_2 ,which is a regulator and $Judger_3$. The value from the PI_2 is sent back to the virtual voltage regulator module as *dE*. $Judger_3$ selects the subsequent input value according to the interval where the difference is located, similar to $Judger_4$. In terms of frequency, it is judged according to the difference between the two sides. The pre-synchronization phase ends, when all three Judgers are selected as 1, and switch signal is changed from 0 to 1.

The microgrid inverter module is a three-phase full-control bridge structure, and the filter module is an LCL structure, system parameters are shown in Table II.

TABLE 4.1 List of LCL structure components

Components	Values	Components	Values
L_1	6 mH	K_p , k_U	800kW/Hz, 0.8Hz/kVar
L_2	1.5 mH	PWM freq	25kHz
C	6 micro-F	P at constant load	10kW
J	$0.15kg.m^2$	Q at constant load	8kVar
r_a	0.05 ohm	P variable	5kW
X_d	0.05H	Q variable	3 kVar

4.1.1 Numerical Simulations

The grid-connected microgrid is analyzed under 4 different conditions. Initially the microgrid is studied when there is no noise in the system. The economic dispatch algorithm provided in the previous section is tested to see the performance of the system in absence of noise. In the second condition, noise of variance 0.2 is introduced in the system, and the performance is observed. During the third condition, noise variance is increased to 0.5 and for the final condition; the noise variance is set to 0.8. The performance of the microgrid under different noise conditions with and without VSG control strategy has been analyzed using MATLAB. In all the cases, power output of the 4 generator units tries to maintain its optimal dispatch schedule with the introduction of different noise levels. In the end, a comparison has been made to show how the system stabilizes the incremental cost under various noise conditions. Fig. 4.7 shows varying power output of the 4 generator units under 60 sec period without VSG. This case is simulated under noise free conditions. It takes around 20 sec for the system to reach a constant generating power output for high noise variance. Fig. 4.8 shows varying power output of the 4 generator units under 60 sec period with VSG which takes about 5 sec less to reach constant output power for the system.

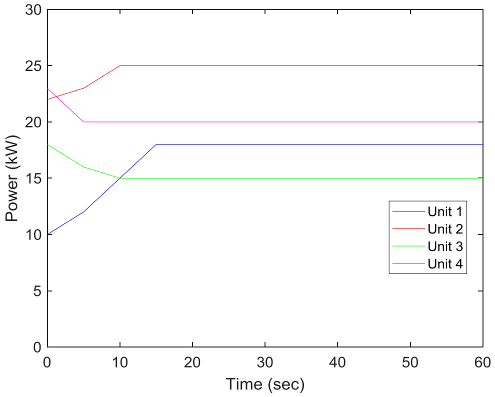

Fig. 4.7 Output power of generator units in kW without noise and VSG

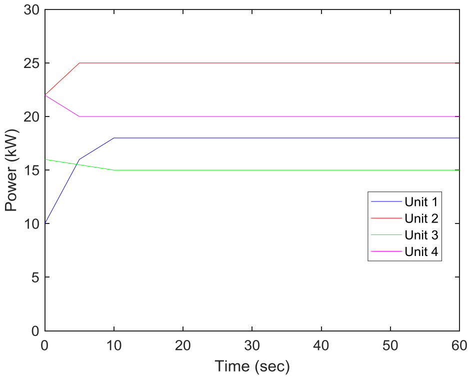

Fig. 4.8 Output power of generator units in kW without noise with VSG

Fig. 4.9, Fig. 4.10 and Fig. 4.11 shows output during some noise variance. In this study, we have considered small (variance of 0.2), medium (variance of 0.5) and large (variance of 0.8) noise levels to simulate the system and observe its behavioral pattern for the chosen consensus-based algorithm. Due to less stability of the system for higher noise levels, the economic dispatch solution changes and is not as stable as observed for lesser noise levels. In all the figures below, it is visible that the system takes a couple of seconds to reach a constant value.

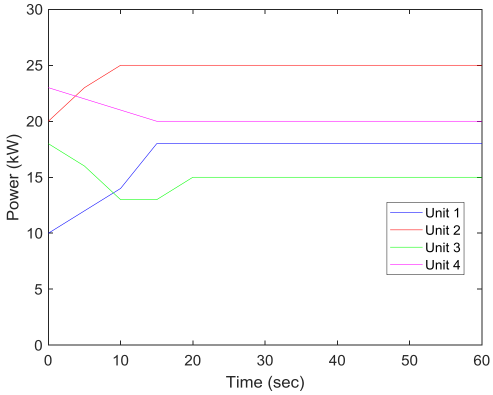

Fig. 4.9 Output power of generator units in kW with 0.2 noise variance without VSG

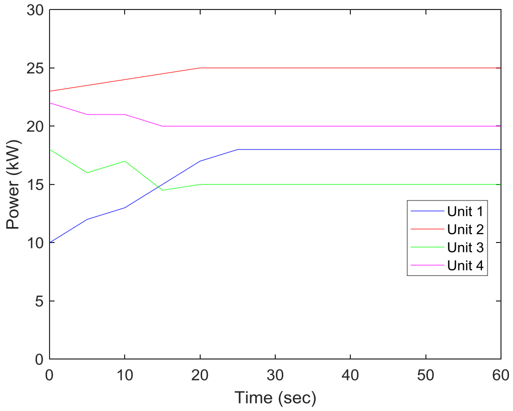

Fig. 4.10 Output power of generator units in kW with 0.5 noise variance without VSG

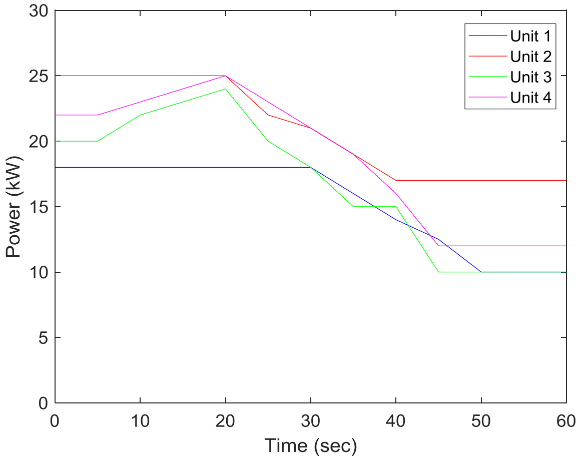

Fig. 4.11 Output power of generator units in kW with 0.8 noise variance without VSG

The higher the noise, the more time it is taken by the system to reach to the desired value. For noise variance of 0.2, the system takes about 20 sec to reach its desired output. For 0.5 noise variance, it takes around 25 sec and 45 sec for 0.8 noise variance.

During no noise condition, the algorithm helps set the incremental cost of all the generator units at a faster pace. With increase in noise variance, it takes time to reach to consensus. But for smaller and medium noise levels, the algorithm worked effectively in weeding out noise in the system.

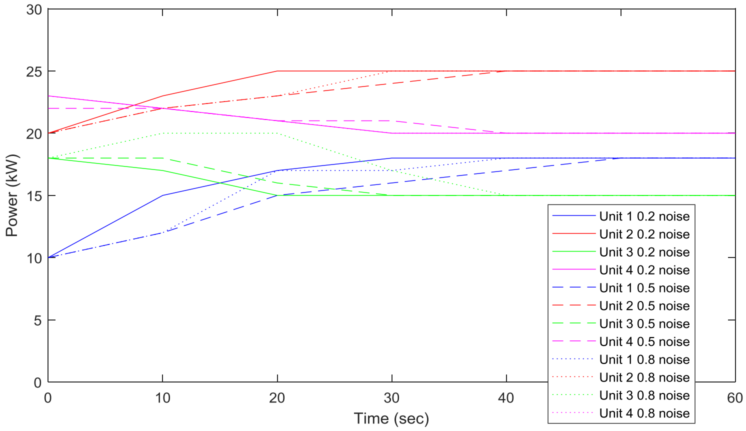

Fig. 4.12 Output power of generator units in kW with all noise variance with VSG

Fig. 4.12 shows varying power output of the 4 generator units under 60 sec period with VSG for all noise variance which takes about 5-10 sec less (compared to without VSG strategy) to reach constant output power for the system. It takes about 5 sec lesser for low and medium level noise and about 10 sec for higher noise variances. The average incremental cost ($/kWh) comes out to be around 5.91 as seen from the graphs, which is close to the values calculated manually.

From Fig. 4.13 and 4.14 it can be seen that with VSG strategy generator units with higher noise level stabilize quicker. It takes on an average 0.45 sec for the system to stabilize with high noise level. This average time decreases with decrease in noise level. Also, in Fig. 4.15 and Fig. 4.16 it was observed that with load change the system is more stable and reaches its maximum limit faster with VSG strategy. The system oscillates more and has more THD without VSG as observed from Fig. 4.15.

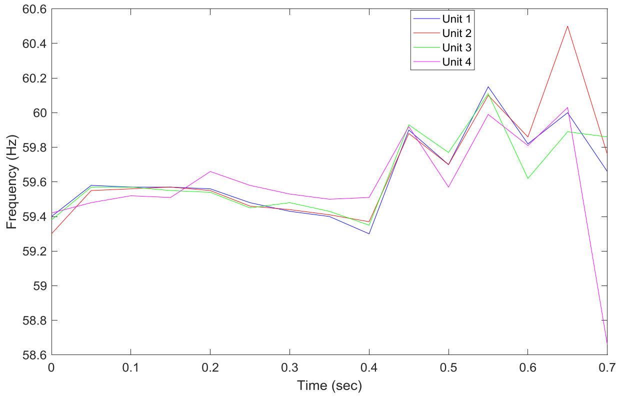

Fig. 4.13 Comparison of frequency change of generator units with 0.8 noise variance without VSG

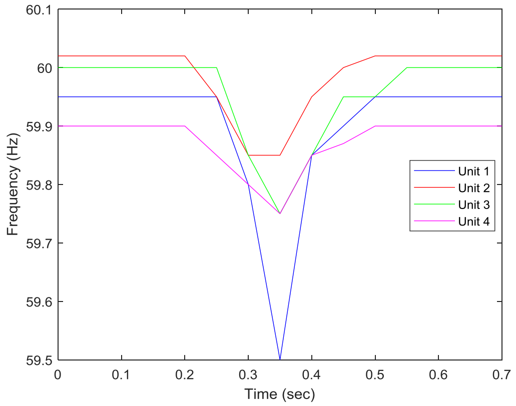

Fig. 4.14 Comparison of frequency change of generator units with 0.8 noise variance with VSG

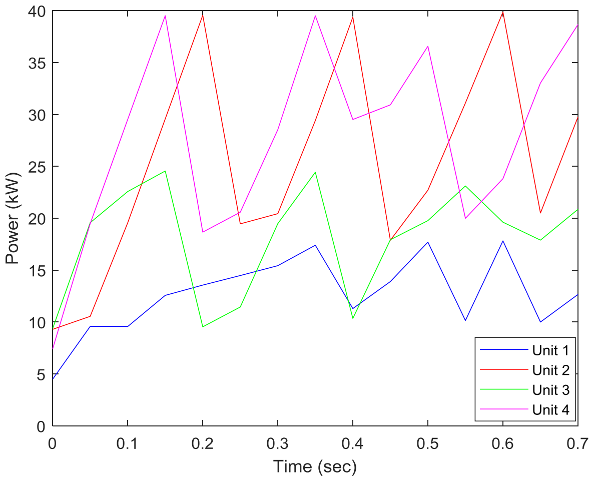

Fig. 4.15 Comparison of maximum power of generator units with 0.8 noise variance and load change without VSG

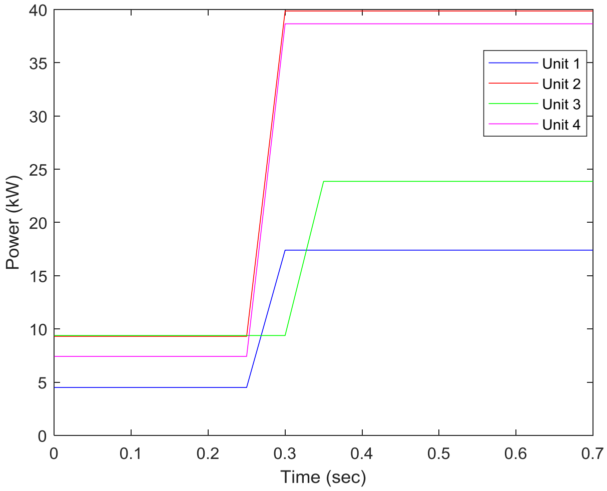

Fig. 4.16 Comparison of maximum power of units with 0.8 noise variance and load change with VSG

4.2 Reactive Power Compensation and STATCOM controller

Most cases consider only active power stability during analysis. However, it is necessary to include reactive power in the analysis to provide an overall stability to the system. Reactive power irregularities are an important factor to be considered. [97]- [100] have used different methods to solve economic dispatch problem. [101]-[104] study consensus based algorithm. Demand side management has been introduced and studied in [105]-[111]. Effects of noise have been considered in [112]-[115]. Distributed approach i.e. central controller is not used in [116]-[121] to solve the economic dispatch problem. FACTS devices have been predominantly used to provide compensation for voltage and phase angle instability [122]. This instability in the system could be due to load fluctuations or inherent noise in the system. STATCOMs are one of the commonly used devices for this purpose amongst many others. This dissertation uses STATCOM based controller to provide voltage and phase angle stability to the islanded microgrid during different noise conditions in a short span of time. STATCOM uses voltage source converter to provide shunt compensation in the microgrid system [123]. Another advantage is that it provides less damping, low harmonics, better response and improved voltage profile in the system [124].

STATCOM is also known as static synchronous compensator/condenser. It is a device famously used for voltage regulation. It is a part of FACTS (flexible alternating current transmission system) family used to increase power transfer capability and improved controllability of the transmission system. It does so by supplying reactive power to the microgrid. A PI (proportional integral) controller is used in conjunction with the STATCOM. PI controller helps reduce voltage flicker in the system [125-127].

Although static var compensation can also be used for voltage stability, STATCOM has better characteristics because it exhibits constant current characteristic during voltage lower than its predefined low limit. STATCOM's are expensive than static var compensation but have low harmonics and faster response. Fig. 4.17 provides the model of STATCOM with PI controller [134-135]. α is the angle of output voltage.

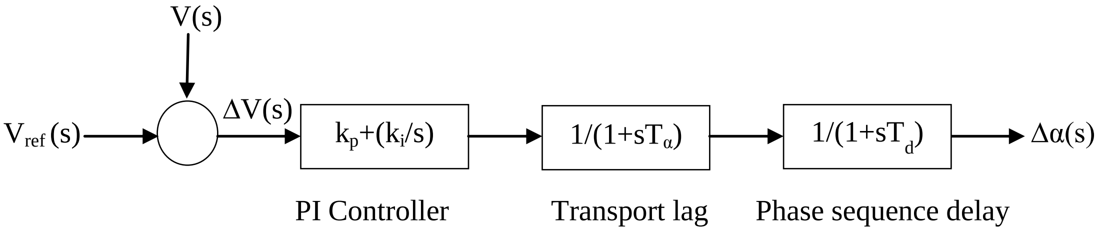

Fig. 4.17 Transfer function model of STATCOM with PI controller [126]

The microgrid under analysis for this section consists of 3 generator units. It is in islanded mode and has a solar/Photovoltaic (PV) generator, wind (doubly fed induction generator-DFIG) generator and a steam turbine unit as shown in Fig. 4.18. Consumer load is assumed as a delta-connected load. STATCOM provides reactive power required to maintain balance in the microgrid. This balance is required due to change in PV generation, change in wind generator output (due to change in wind speed), reactive power load and inherent noise in the microgrid's components. A balance equation for reactive power of the figure below is formulated. The reactive power balance equation is formulated using the following assumption: Reactive power is fed by the STATCOM, PV system and steam turbine unit into the bus and reactive power is sent to the Consumer load and Wind system from the bus.

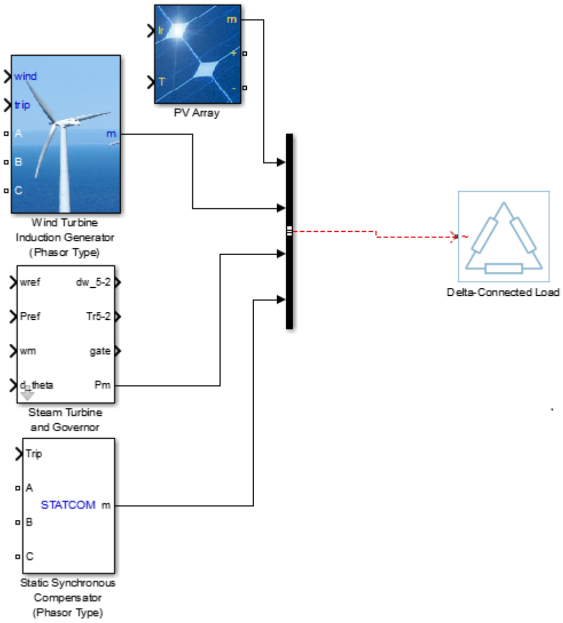
Ir
T
m
+
-
PV Array
wind
trip
A
B
C
m
Wind Turbine
Induction Generator
(Phasor Type)
Delta-Connected Load
wref
Pref
wm
d_theta
dw_5-2
Tr5-2
gate
Pm
Steam Turbine
and Governor
Trip
A
B
C
STATCOM
m
Static Synchronous
Compensator
(Phasor Type)

Fig. 4.18 Microgrid structure including PV, Wind Generator, Steam Turbine and STATCOM Controller as bus inputs and Delta connected load as output from the bus

Table III provides the parameter's values for various generators used in this paper's analysis. Cost-coefficients, minimum and maximum power generation limits of the units are provided below.

TABLE 4.2 List of parameters for generators

Unit	P_{min}(kW)	P_{max}(kW)	a	b	c
1 (PV)	4	18	0.070	2.15	56
2 (Wind)	8	40	0.080	1.15	50
3 (Steam)	5	25	0.070	3.3	41

The reactive power balance equation is written as follows:

$$\Delta Q_{PV} + \Delta Q_{ST} + \Delta Q_{STATCOM} = \Delta Q_L + \Delta Q_{IG} \tag{15a}$$

Change in load or noise level, changes the terminal voltage which in turn changes the reactive power output of the different microgrid components. This changes the output voltage of microgrid [126]:

$$\Delta V(s) = \frac{K_v}{1+sT_v}[\Delta Q_{PV}(s) + \Delta Q_{ST}(s) + \Delta Q_{STATCOM}(s) - \Delta Q_L(s) - \Delta Q_{IG}(s)] \tag{15b}$$

Where,

$\frac{K_v}{1+sT_v}$ is the derivative of different components' reactive output power with respect to time and voltage.

The primary objective of this analysis is to make the system more stable under noise conditions and reduce damping in the microgrid system. Voltage stability margin is achieved by minimum increment in terminal voltage of the system and less damping in the system. Integral absolute error (IAE), Integral square error (ISE), Integral square time error (ISTE) are some performance indexes used to reduce overshoot, settling time, rise time, steady-state error of the terminal voltage. Table IV provides values of these parameters for PI controller used with the STATCOM.

TABLE 4.3 Parameter values for PI controller

System parameter	PI Controller
K_p	61
K_i	13000
IAE	960
ITSE	23
ITAE	16

Rise time	0.09
Overshoot	0.02

It is anticipated that the VSG and STATCOM control strategies have same initial state. They are also subjected to the same disturbance and reach the steady state. The difference offset ratio D1-0% and the optimization percentage Dn-s% are used for parameter evaluation criteria. D1-0% is the ratio of difference between the parameter offsets under two strategies and the initial value, which represents the degree of decrease of new strategy offset relative to standard strategy offset. It is given as:

$$D_{1\text{-}0}\,\% = \frac{|A_{1s} - A_0| - |A_{1n} - A_0|}{A_0} \times 100\% \tag{16}$$

Dn-s% represents the parameter optimization degree of the new strategy relative to the standard strategy.

$$D_{n\text{-}s}\,\% = \pm\frac{A_{1s} - A_{1n}}{A_{1s}} \times 100\% \tag{17}$$

where the ‘±’ is determined by the character of the specific parameter.

4.2.1 Numerical Simulation for Lagrange method

Initially the microgrid is studied when there is no noise in the system. The economic dispatch algorithm provided in the previous section along with reactive power compensation is tested to see the performance of the system in absence of noise. In the second condition, noise of variance 0.2 is introduced in the system, and the performance is observed. During the third condition, noise variance is increased to 0.5 and for the final condition, the noise variance is set to 0.8. The performance of the microgrid under different noise conditions has been analyzed using MATLAB. In all the cases, power output of the 3 generator units tries to maintain its optimal dispatch schedule with the introduction of different noise levels.

Fig. 4.19 shows comparisons between terminal voltage of the microgrid system with respect to time under different noise conditions. As seen from the graph, higher noise variance (purple legend) is not easy to stabilize the microgrid during islanded mode, and takes time to stabilize itself. Reactive power compensation helps stabilize the system very fast for low to medium level noise. This can be also be concluded from the graph by looking at the red, black, and pink legends with correspond to no noise, low and medium noise variance respectively. For phase angle stability, it is observed that with only use of economic dispatch algorithm for optimal schedule, the system takes longer to stabilize itself. This leads to a less stable, low efficient and slow response microgrid system. With addition of reactive power compensation, the system gives faster response and is more stable. In power systems, it is important for a system to be resilient and have faster response because load keeps changing most of the time and is hardly ever constant. Hence, it is important for a system to be ready to take up these challenges and be more resilient. This consensus based economic dispatch algorithm in conjunction with STATCOM based reactive power compensation provides the necessary stability and resiliency.

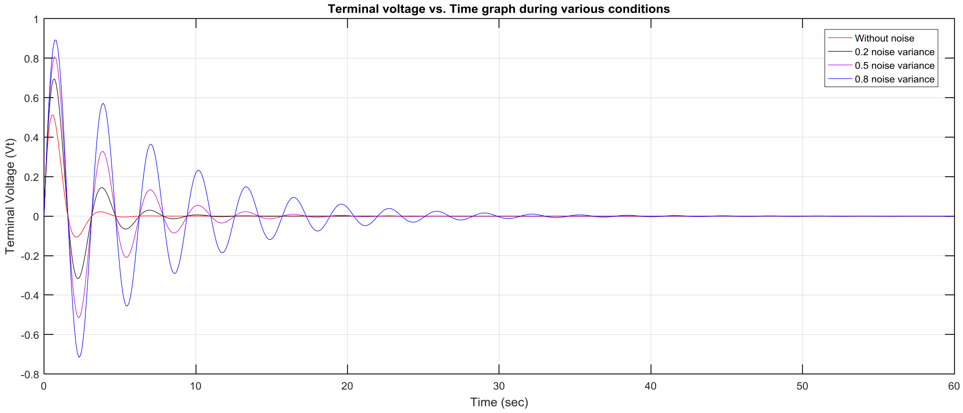

Fig. 4.19 Comparison of terminal voltage for all noise conditions

Similar analysis is done when STATCOM controller is used in conjunction with VSG strategy to observe voltage and frequency fluctuations in the system.

After 0.4 seconds of stable operation of microgrid with constant load, the variable load is connected, and removed at 0.7 seconds. Fig. 4.20 – Fig. 4.24 is a comparison diagram of output voltage, system frequency, output active power, and output reactive power of STATCOM controller with and without VSG control strategy.

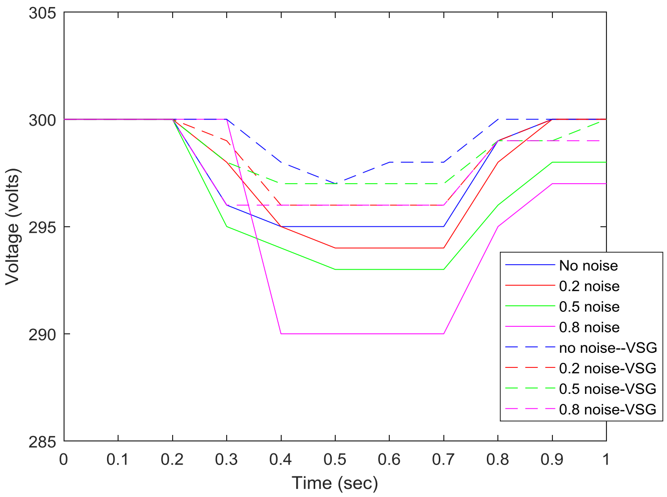

Fig. 4.20 Voltage fluctuations for all noise variances with and without VSG

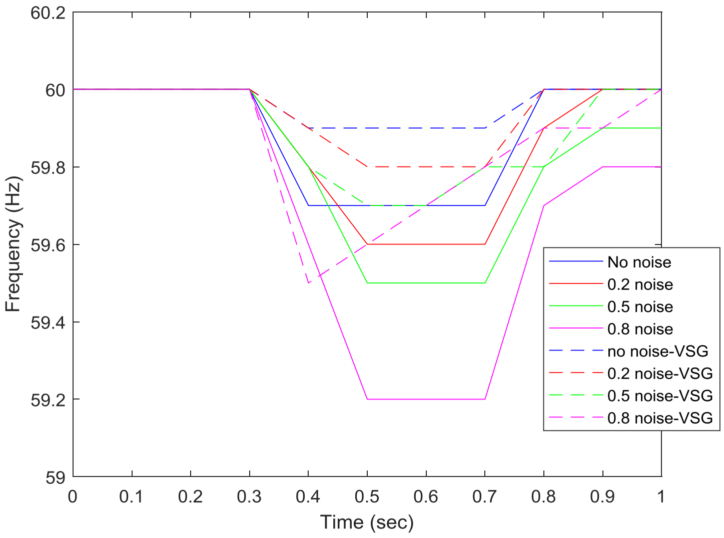

Fig. 4.21 Frequency fluctuations for all noise variances with and without VSG

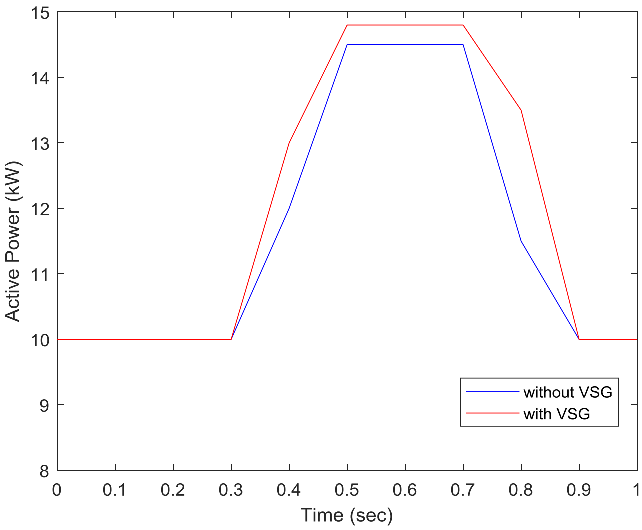

Fig. 4.22 Comparison of Active power for no noise

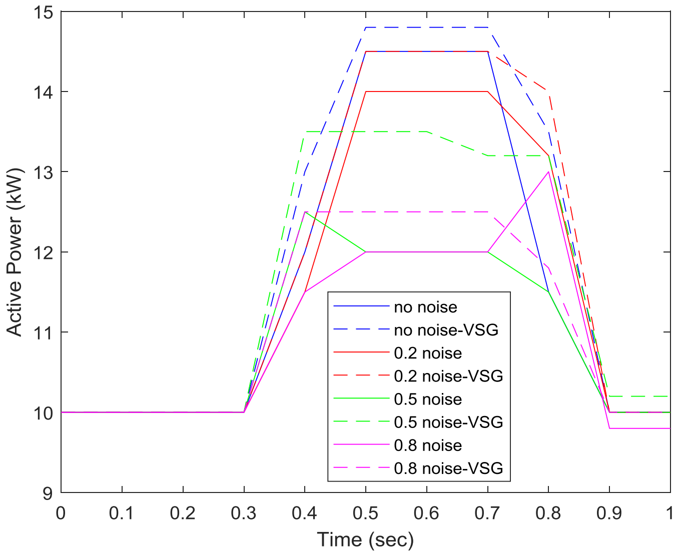

Fig. 4.23 Active power for all noise variances with and without VSG

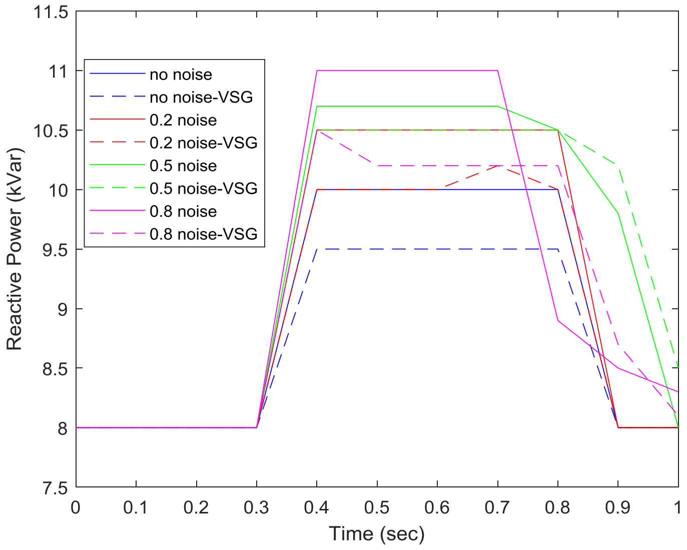

Fig. 4.24 Reactive power for all noise variances with and without VSG

It can be seen from Fig. 4.20 that when variable load is connected, the output voltage under VSG control strategy drops from 300V, however the system drops lesser as compared to without VSG for all noise levels. Similar observation is made from Fig. 4.21 for frequency.

The output active power is 14 kW, and the output reactive power is 10 kVar with VSG strategy. The output active power is 12.6kW, and the output reactive power is 9.5kVar.

Table V provides difference offset ratio D $_{1\text{-}0}$ % for both with and without VSG cases. From the table, it is evident that the reactive power compensation is more when STATCOM-VSG strategy is used for all noise variances in the system.

Table 4.4 D $_{1\text{-}0}$ % with and without VSG cases

Parameters	Initial Value	Without VSG	With VSG	$D_{1\text{-}0}$ %
Voltage	300 V	292 V	298 V	2 %
Frequency	60 Hz	59.4 Hz	59.8 Hz	0.67 %
Active Power	10 kW	13.3 kW	14 kW	7 %
Reactive Power	8 kVar	10.5 kVar	10 kVar	-6.25 %

4.3 Network figure and single line diagram of system

Fig. 4.25 constitutes the network figure. Incremental costs from each generator are shared with agents. These agents share data with each other and decide if it’s the optimal incremental cost. If not, the information is passed on to the generator to adjust its output power until optimal incremental cost criterion is met. Once optimal economic dispatch solution is found, the total output power is sent to VSG which is then used to meet load demand or sent to grid to fulfill any power deficit. The use of consensus-based algorithm and VSG strategy helps reduce the noise effects and stabilize the microgrid. With the introduction of various noise levels, the power output of the four generating units is observed and tries to imitate the ideal dispatch schedule in all instances. To demonstrate the system's stability and the incremental cost for varied noise levels, a comparison has been prepared.

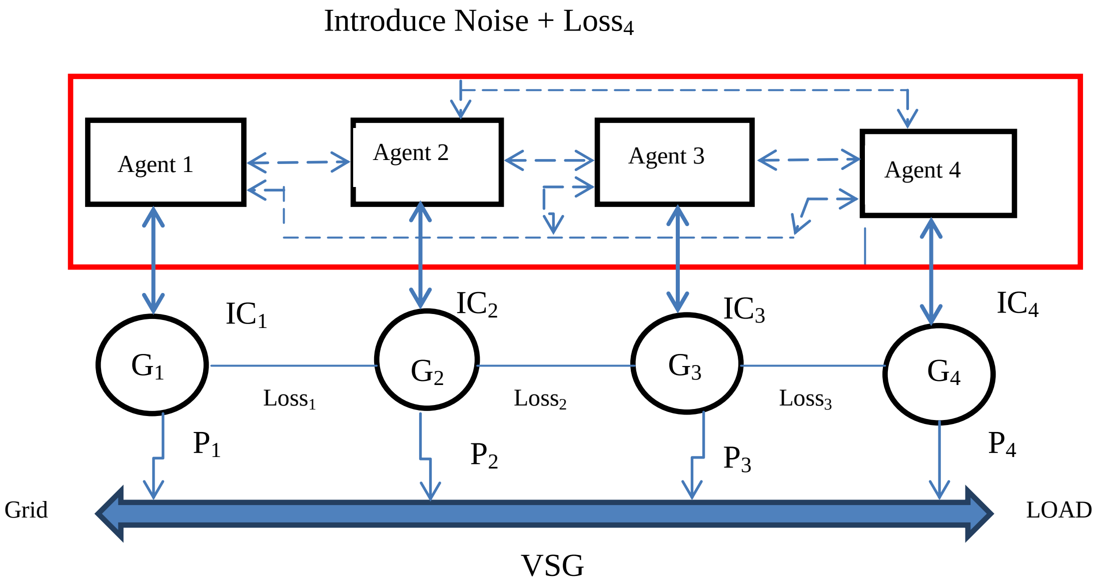
Introduce Noise + $Loss_4$
Agent 1
Agent 2
Agent 3
Agent 4
IC_1
IC_2
IC_3
IC_4
G_1
G_2
G_3
G_4
$Loss_1$
$Loss_2$
$Loss_3$
P_1
P_2
P_3
P_4
Grid
LOAD
VSG

Fig. 4.25 Network figure

Single line diagram of the system is provided below in Fig. 4.26 to explain the system under study consisting of three generators (PV, wind turbine, and steam turbine). The power generated from the generators is first conditioned using consensus-based algorithm to include noise and load variation. This conditioned power (VI) is then sent to the VSG control system and PI controller-based STATCOM. This optimal active power and compensated reactive power is then fed to SPWM. The conditioned power is sent to the loads via inverter and PCC.

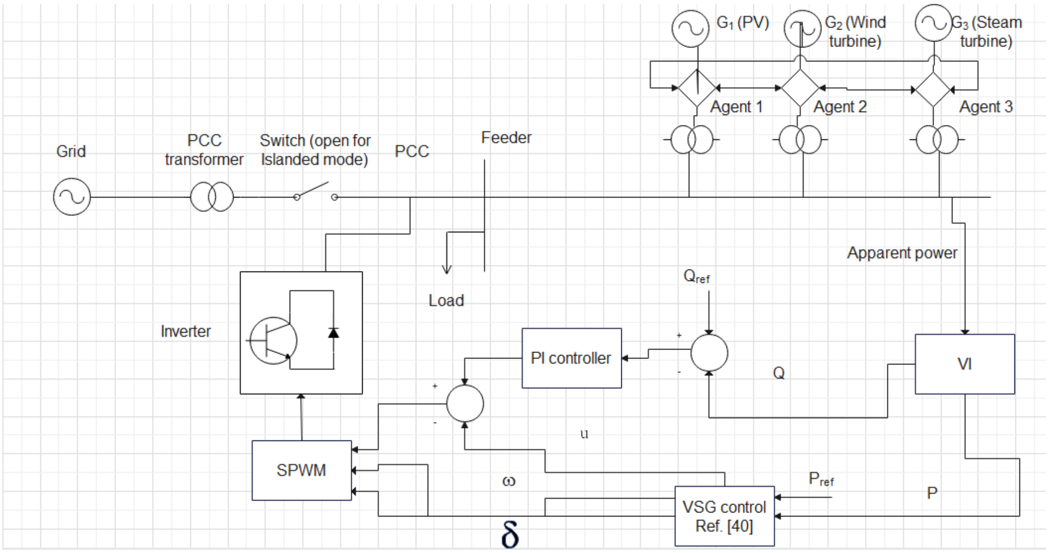
G1 (PV)
G2 (Wind turbine)
G3 (Steam turbine)
Agent 1
Agent 2
Agent 3
Grid
PCC transformer
Switch (open for Islanded mode)
PCC
Feeder
Apparent power
Qref
Load
Inverter
PI controller
Q
VI
+
-
u
SPWM
ω
Pref
P
VSG control Ref. [40]
δ

Fig. 4.26 Single line diagram of system

4.4 Discussions

It can be concluded from Fig. 4.23 that there is a shift in economic dispatch solution due to large variance in noise. During no noise condition, the system takes less than 20 sec to reach constant power output. The system takes 25 sec for 0.2 noise variance, around 40 sec for 0.5 noise variance and 50 sec for 0.8 noise variance to reach constant power output.

The proposed consensus based algorithm for economic dispatch works well for islanded microgrids [93]. In this section, this proposed algorithm was used to analyze the behavior of microgrid during islanded A mode in conjunction with STATCOM based reactive power compensation. The microgrid shows good response for different noise levels when reactive power is compensated in the system. It brings the system close to constant output power in less time. However, it was observed that it took longer for the system to reach its desired stability without any reactive power compensation. The system had more harmonics and oscillations for a longer time and hence can be said that it took longer to achieve stability. It can be concluded from this study, that this consensus based economic dispatch algorithm with reactive power compensation is very good for islanded microgrids during small, medium, and large variance noises. It provides stability, efficiency, and resiliency to the system in a short span of time based on the case study.

With inclusion of VSG control strategy the system is able to stabilize much faster in the event of noise and load changes as seen from the results section. In islanded-mode of operation, the performance of VSG control strategy with STATCOM controller on voltage, frequency, active power, reactive power, are better than using only STACOM controller.

Chapter 5. Comparison Results of different Algorithm

5.1 Comparison between Lagrange and PSO algorithms for active power

Four different scenarios are used to examine the grid-connected microgrid. When there is no noise present in the system, the microgrid is initially evaluated. The preceding section's Lagrange method and PSO algorithm are evaluated to see how well it operates in the absence of noise. In the second scenario, the system is subjected to noise with a variance of 0.2, and the performance is tracked. The noise variance is raised to 0.5 for the third test, and it is set to 0.8 for the final condition. MATLAB has been used to examine how well the microgrid performs under various noise circumstances with and without the VSG control approach.

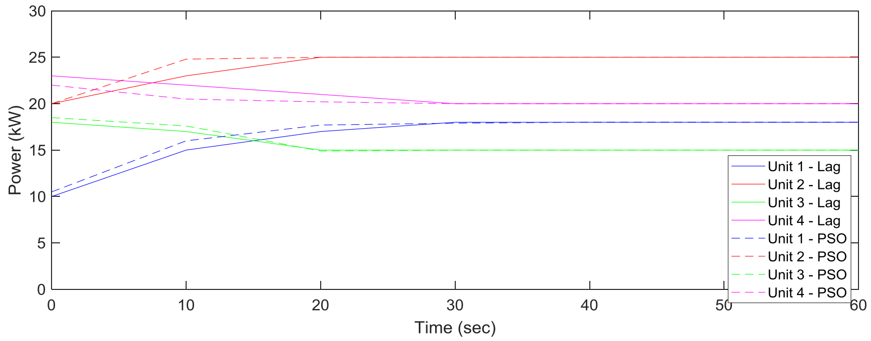

Fig. 5.1 Comparison of generator units' output power in kW with 0.8 noise levels for Lagrange and PSO algorithm using VSG

Fig. 5.1 compares the output power of all generating units for 0.8 noise level using the Lagrange method and PSO algorithm with the VSG control strategy. The resulting graph shows that PSO performs better than Lagrange. With the PSO algorithm convergence occurs faster than the Lagrange method. For Unit 1, PSO achieves stability 3 sec earlier at the 27-sec mark. For unit 2, PSO performs better by 10 sec as seen from the red legend. For Units 3 and 4, PSO performs slightly better than the Lagrange method. The processing time for the PSO algorithm was 15.648 sec whereas it took 22.343 sec for the Lagrange method. Overall, it can be concluded that the PSO algorithm solves the economic dispatch problem much quicker and efficiently.

Table VI compares the Lagrange method and PSO algorithm performance when used with the VSG control strategy for incremental cost criterion. For all noise variances, PSO performs better and provides quicker stability. For no noise conditions, PSO takes 27.45 sec to reach optimal incremental cost whereas the Lagrange method takes about 38.21 sec. With 0.2 noise variance, PSO takes 10 sec less than the Lagrange method to reach optimal incremental cost. For a medium noise variance of 0.5, PSO is faster by about 13 seconds and about 39 seconds faster for high noise variance of 0.8. It is observed from Table VI that PSO performs better for all levels of noise variance and takes much less time to stabilize the system.

Table 5.1 Comparison of time to reach average optimal incremental cost for both methods

Noise variance	Lagrange method	PSO Algorithm
No noise	38.21 sec	27.45 sec
0.2 variance	48 sec	38.20 sec
0.5 variance	52.57 sec	40.19 sec
0.8 variance	90 sec	51.85 sec

Table VII compares the Lagrange method and PSO algorithm performance when used with VSG control strategy for frequency and maximum power. For all noise variances PSO performs better and provides quicker stability. For 0.8 noise condition, PSO takes 0.2 sec to frequency stability whereas Lagrange method takes about 0.45 sec. Similarly, for maximum power PSO algorithm takes half the time to reach stability as seen from Table VII.

Table 5.2 Comparison of time to reach optimal levels of parameters for 0.8 noise variance

Method/Algorithm	Frequency (Hz)	Max. Power (kW)
Lagrange	0.45 sec	0.30 sec
PSO	0.20 sec	0.15 sec

5.2 Comparison between Lagrange, Firefly, and ABC algorithms for economic dispatch and reactive power compensation

MATLAB is used for this study’s simulations. When there is no noise present in the system, the microgrid is initially evaluated. To assess how well the system performs in the absence of noise, the preceding section's economic dispatch algorithms are used coupled with reactive power compensation. The system is subjected to noise with a level of 0.2 variance to compare its performance. The noise level is raised to 0.5 variance during the third condition and to 0.8 variance during the final condition. With the inclusion of various noise levels, load variation at 0.3 sec is introduced in the system. This load varies due to changes in load demand. The output power of the three generator units seeks to preserve its ideal dispatch schedule in all instances. Fig. 5.2-Fig. 5.4 compares incremental cost (IC) for the three generating units. For Lagrange method, it takes about 60 s to reach the optimal IC of 6 $/kWh. Whereas in Firefly and ABC algorithms, it takes about 55 s and 50 s respectively, to reach the optimal value. ABC algorithm outperforms the two in terms of IC in islanded microgrid.

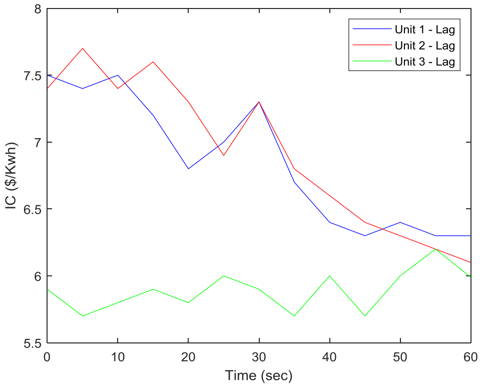

Fig. 5.2 Comparison of incremental cost of units using Lagrange method with VSG-STATCOM strategy

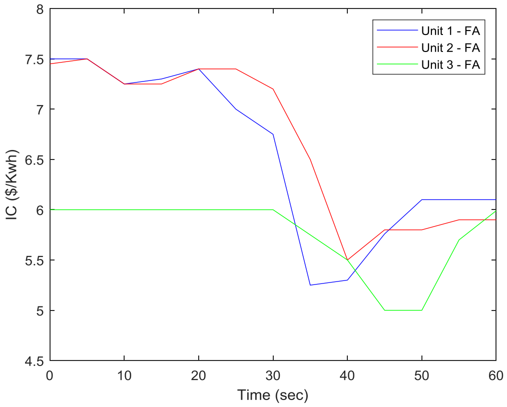

Fig. 5.3 Comparison of incremental cost of units using FA algorithm with VSG-STATCOM strategy

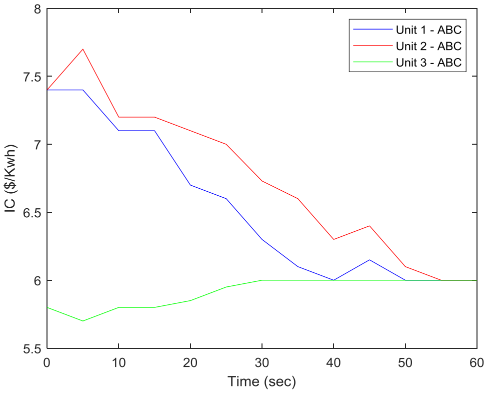

Fig. 5.4 Comparison of incremental cost of units using ABC algorithm with VSG-STATCOM strategy

Fig. 5.5- Fig. 5.8 compares the microgrid system's voltage fluctuations with respect to time for the three different algorithms. The system is compared for all noise levels (no noise, 0.2, 0.5, and 0.8 noise variance) with and without VSG control strategy. It can be concluded that for all cases, the inclusion of VSG helps control the fluctuations much faster. In most cases, it takes about 0.85 sec to reach stability. However, it can be seen that the ABC algorithm (green legend) outperforms other algorithms and reaches stability faster in all noise variance. Also, the voltage fluctuations are observed to be low in ABC algorithm compared to Firefly and Lagrange methods. It is also observed that most units reach 300 volts faster and with fewer fluctuations when the ABC-VSG strategy is used (green dashed line legend).

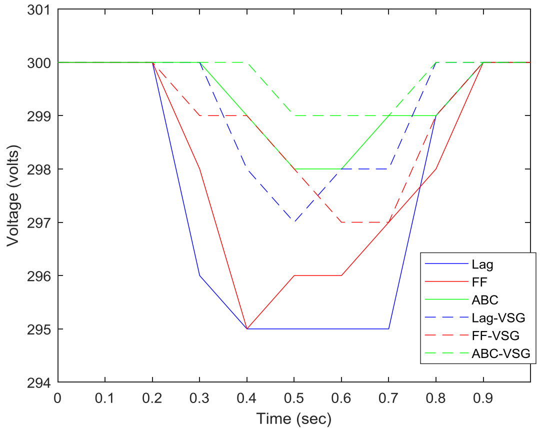

Fig. 5.5 Comparison for Voltage fluctuations for no noise with and without VSG

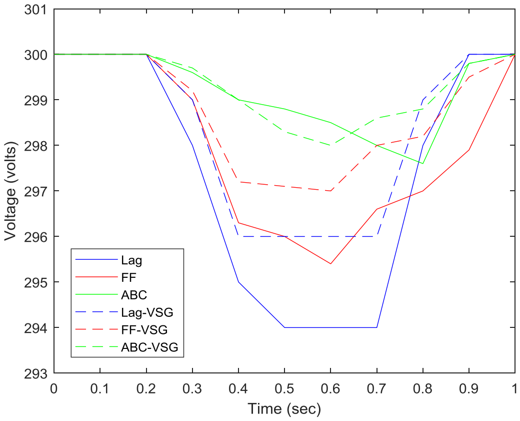

Fig. 5.6 Comparison for Voltage fluctuations for 0.2 noise level with and without VSG

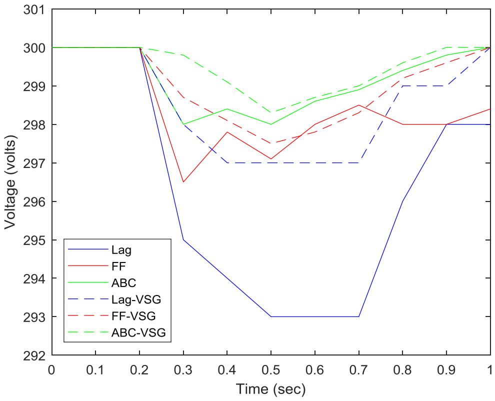

Fig. 5.7 Comparison for Voltage fluctuations for 0.5 noise level with and without VSG

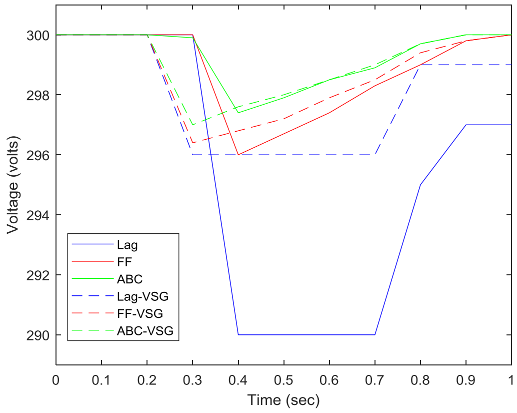

Fig. 5.8 Comparison for Voltage fluctuations for 0.8 noise level with and without VSG

A similar conclusion can be drawn for frequency fluctuations from Fig. 5.9-Fig. 5.12. The average time taken to reach 60 Hz frequency is about 0.75 sec in ABC algorithm when used with VSG for all noise variances. For other cases, the time taken to reach a stable value of 60Hz is more as seen from the graphs. Moreover, the frequency fluctuations are less for ABC-VSG strategy (green dashed line legend).

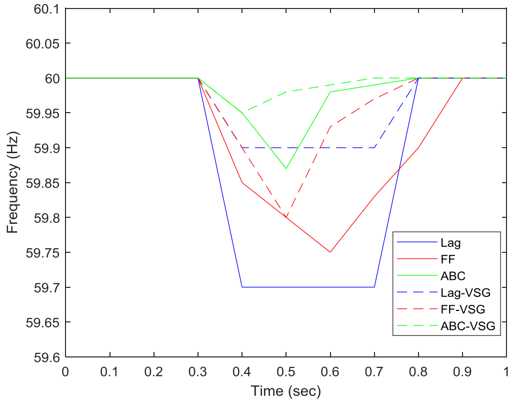

Fig. 5.9 Comparison for Frequency fluctuations for no noise condition with and without VSG

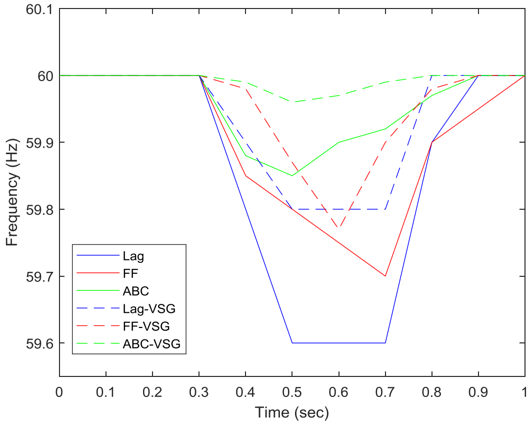

Fig. 5.10 Comparison for Frequency fluctuations for 0.2 noise level with and without VSG

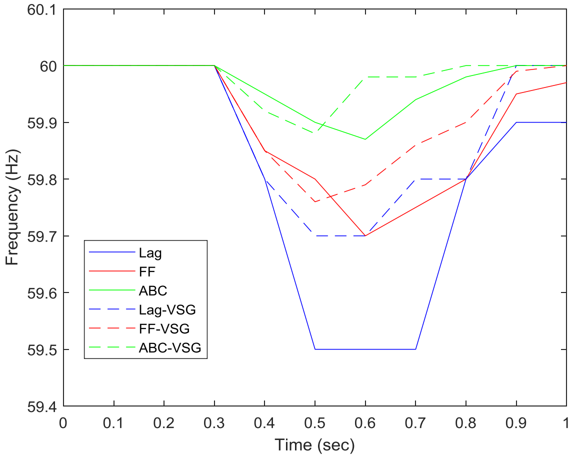

Fig. 5.11 Comparison for Frequency fluctuations for 0.5 noise level with and without VSG

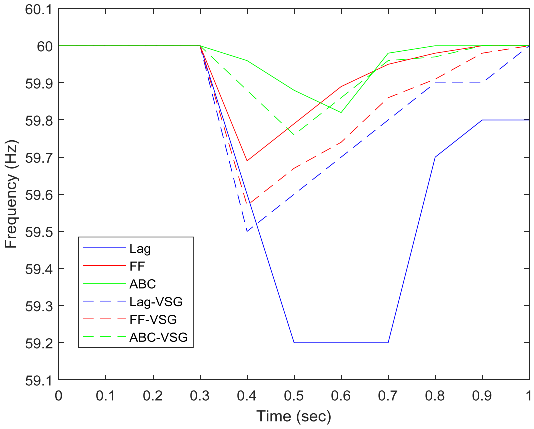

Fig. 5.12 Comparison for Frequency fluctuations for 0.8 noise level with and without VSG

Fig. 5.13 compares the microgrid system's active power fluctuations with respect to time using Lagrange method. It is observed that there is more fluctuation in the system with higher noise variance. But the addition of VSG technology helps in better transition and much smoother functioning of the system. On average, it takes about 0.9 sec for the system to stabilize. Similarly, it is observed from Fig. 50, a high noise level makes it difficult to stabilize the islanded microgrid for the Firefly algorithm and takes about 1 sec for most cases. Again VSG performs better with this algorithm. ABC algorithm's performance is shown in Fig. 51. It can lower fluctuations for all noise variances at a faster rate of about 0.7 sec on average than other algorithms. It also performs better when used with the VSG control strategy.

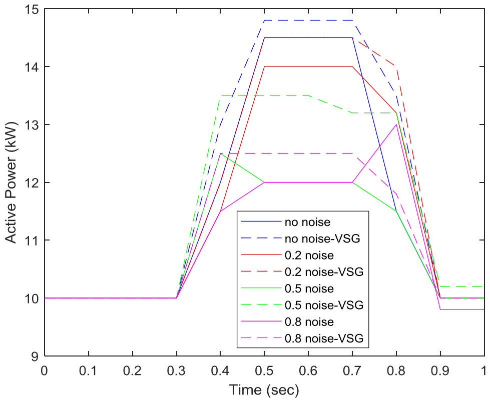

Fig. 5.13 Active power for all noise variances with and without VSG for Lagrange method

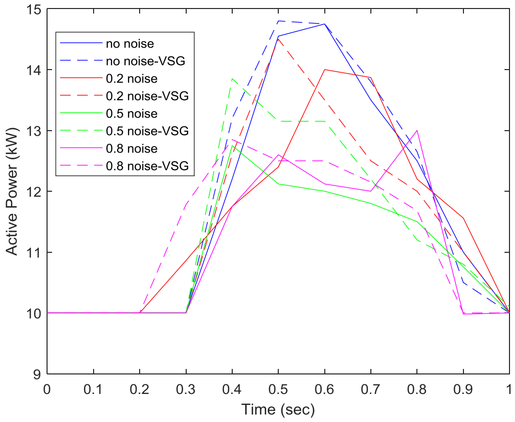

Fig. 5.14 Active power for all noise variances with and without VSG for Firefly algorithm

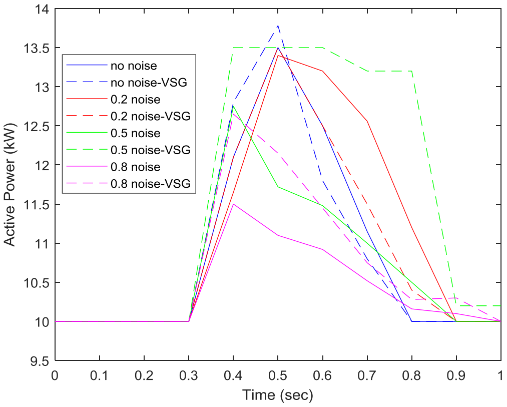

Fig. 5.15 Active power for all noise variances with and without VSG for ABC algorithm

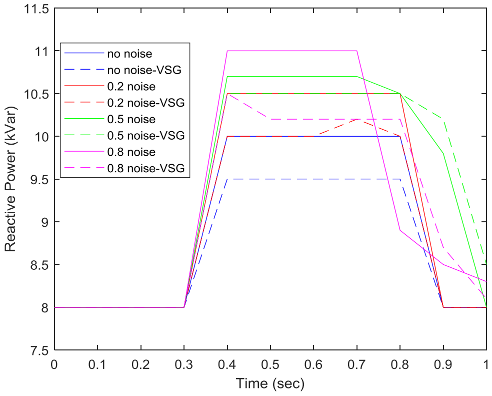

Fig. 5.16 Reactive power for all noise variances with and without VSG for Lagrange method

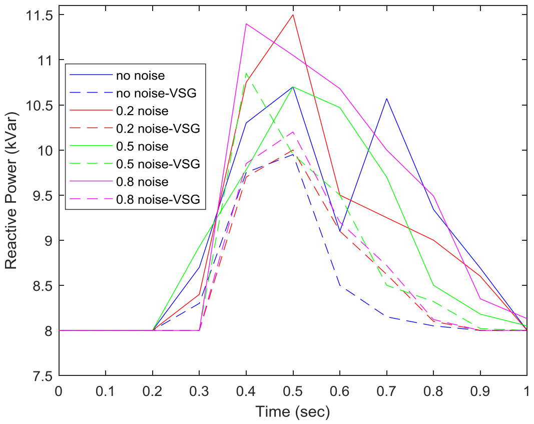

Fig. 5.17 Reactive power for all noise variances with and without VSG for Firefly algorithm

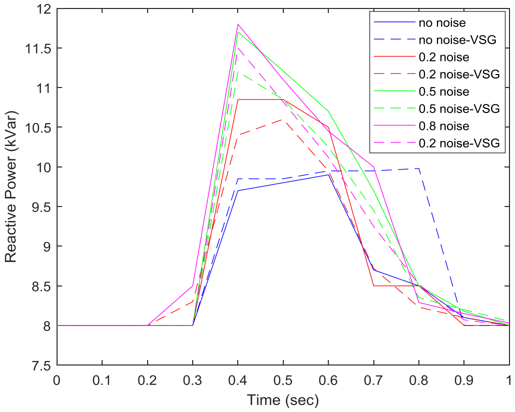

Fig. 5.18 Reactive power for all noise variances with and without VSG for ABC algorithm

Fig. 5.16 – Fig. 5.18 compares the reactive power response for all algorithms and it can be concluded that with higher noise variances, it gets difficult to manage reactive power compensation. However, with the STATCOM-VSG strategy, compensation performance increases in all three algorithms. It is observed that Lagrange and ABC methods work slightly better than the Firefly algorithm. It takes less than 1 sec to compensate for reactive power in Lagrange and ABC algorithms. As seen from Fig. 53, it will take more than 1 sec for the system to compensate optimal reactive power value of 8

kVar for Firefly algorithm. In all cases, it was observed that the ABC algorithm response rate is higher than Lagrange and Firefly algorithms.

Table VIII provides the initial values to calculate the difference offset ratio for Lagrange formulation. As demonstrated in Fig. 5.5-5.8, the output voltage under the VSG control strategy decreases from 300 volts when a variable load is attached, but the voltage fluctuates less with the VSG-STATCOM strategy for all noise levels. A similar finding for frequency is drawn from Fig. 5.9-5.12 for frequency. With the VSG strategy, the output active power is 14 kW, and the output reactive power is 10 kVar. The differential offset ratio D_{1-0}% for different algorithms is shown in Table VIII-X for both scenarios with and without VSG. The tables' results show that using the STATCOM-VSG technique for all system noise variations results in greater reactive power compensation. The difference offset ratio for voltage is 2% in Lagrange method, 0.83% in Firefly algorithm, and 0.5% in ABC algorithm. For frequency parameter, it is 0.67% in Lagrange, 0.33% in Firefly, and 0.13% in ABC algorithm. Similarly, for active and reactive power the difference offset ratio is the least in ABC algorithm and highest in Lagrange method. Settling time of 0.79 s is found to be least in ABC algorithm. Firefly algorithm settles at 0.92 s whereas Lagrange method settles at 0.9 s. Settling time is observed to be lesser with VSG strategy. Similarly, maximum overshoot is least for ABC algorithm with a value of 12.8 kW. Hence, it can be ascertained that the difference offset ratio for various parameters is found to be the least in the Artificial Bee Colony algorithm. Thus, it provides a much more secure, stable, cost-effective, and efficient functionality for microgrids.

Table 5.3 Difference offset ratio for Lagrange method

Parameters	Initial Value	Without VSG	With VSG	D_{1-0} %
Voltage	300 V	292 V	298 V	2 %
Frequency	60 Hz	59.4 Hz	59.8 Hz	0.67 %
Active Power	10 kW	13.3 kW	14 kW	7 %
Reactive Power	8 kVar	10.5 kVar	10 kVar	-6.25 %
Settling time (Power)	-	0.95 s	0.9 s	-
Max. Overshoot (Power)	-	14.8 kW	14.4 kW	-

Table 5.4 Difference offset ratio for Firefly algorithm

Parameters	Initial Value	Without VSG	With VSG	D_{1-0} %
Voltage	300 V	296 V	298.5 V	0.83 %
Frequency	60 Hz	59.75 Hz	59.95 Hz	0.33 %
Active Power	10 kW	13.5 kW	14 kW	5 %
Reactive Power	8 kVar	11.1 kVar	10.7 kVar	-5 %
Settling time (Power)	-	0.98 s	0.92 s	-
Max. Overshoot (Power)	-	14.9 kW	14.5 kW	-

Table 5.5 Difference offset ratio for ABC algorithm

Parameters	**Initial Value**	**Without VSG**	**With VSG**	**D_{1-0} %**
Voltage	300 V	298 V	299.5 V	0.5 %
Frequency	60 Hz	59.9 Hz	59.98 Hz	0.13 %
Active Power	10 kW	13.85 kW	14.25 kW	4 %
Reactive Power	8 kVar	11.5 kVar	11.2 kVar	-3.75 %
Settling time (Power)	-	0.86 s	0.79 s	-
Max. Overshoot (Power)	-	13.5 kW	12.8 kW	-

5.3 Discussions

The microgrid’s performance is compared for both Lagrange and PSO algorithms with and without the use of the VSG strategy. It is concluded that with the inclusion of the VSG control strategy, the system can stabilize much faster in the event of different levels of noise and load changes as seen from the results section. This is observed for both the Lagrange method and the PSO algorithm. The consensus-based economic dispatch algorithm works efficiently in conjunction with the VSG control strategy. It can also be concluded from the results obtained that the PSO algorithm performs better in stabilizing the frequency, output power, and load changes in the microgrid. The optimal incremental cost is also achieved faster in the PSO algorithm.

The three discussed algorithms (Lagrange, Firefly, and ABC) were utilized in this study to examine how the microgrid operates in islanded mode for various noise levels while also providing reactive power compensation. In a shorter time period, it drives the units to desired incremental cost value. ABC algorithm reaches 6 $/kWh IC in about 50 s whereas the other two algorithms take about a minute to reach this value. In case of voltage fluctuations, 300V is reached faster in ABC algorithm in 0.75 sec. For frequency, it takes between 0.75 s to 0.9 s for various noise levels. With a higher noise level of 0.8, it takes longer for frequency to reach 60 Hz for all three algorithms. ABC algorithm provides a faster response of an average of 0.75 s. Similarly for active power and reactive power, ABC algorithm takes less than a second to reach their ideal value, whereas it takes longer for the other two methods to reach the desired value. With the inclusion of VSG control strategy, the system can stabilize much faster in the event of noise and load changes as seen from the results section. In islanded mode, the performance of the VSG control strategy with the STATCOM controller on voltage, frequency, active power, and reactive power parameters is better.

It can also be concluded that the ABC algorithm performs the best among the other algorithms discussed in this paper. It has a quicker response and lesser fluctuations for all four parameters. Hence, the ABC algorithm is best suitable for economic dispatch solution with noise as well as provides a reliable and stable islanded microgrid system.

Chapter 6. Cost study of Microgrids

The Microgrid Cost Study aims at identifying the average cost of a typical microgrid project. The project is limited to the vicinity of U.S. and hence takes into account of only existing microgrid projects in U.S. The project's objective is to find cost of microgrid and its individual components for next 5 years. This will help in R&D for future microgrid projects as well as help investors/developers/researchers get an idea about the cost of their projects that they might want to start in near future. Most of the microgrids are found in sectors such as: commercial, community or campus as shown if Fig. 6.1.

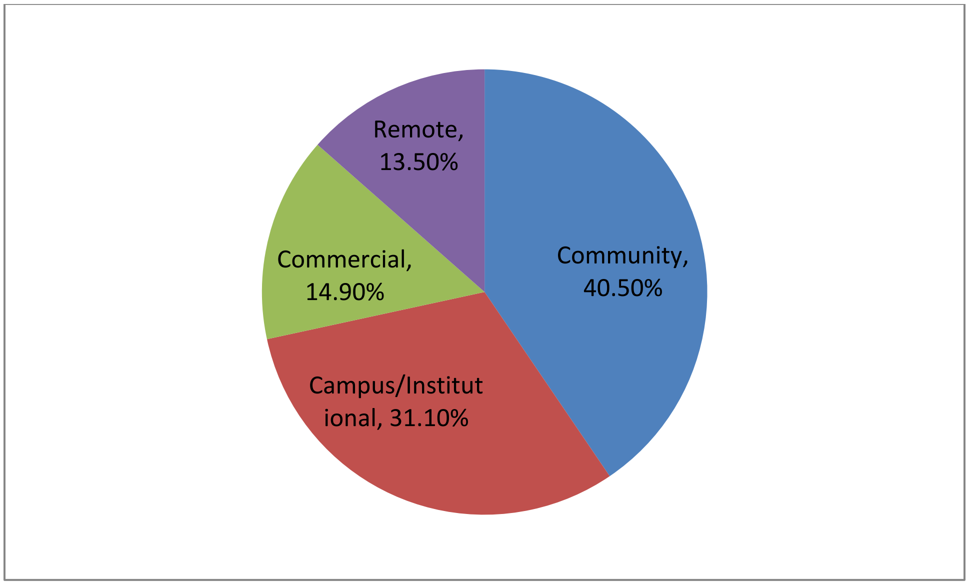

Fig. 6.1 Microgrid Cost Study Project Data by number of Projects

6.1 Importance of cost study

Microgrid brings us not only direct economic benefits but also indirect benefits such as efficiency, reduced emissions, and improved power quality and reliability (PQR). Microgrid is proposed by Consortium for Electric Reliability Technology Solutions (CERTS). The microgrid concept [127-129] heavily depends on the reduction of production costs of renewable energy generation, storage technologies, reliability and flexibility of electric power system, energy management systems and hence able to operate with and without utility grid connection [130]-[131]. Microgrids with distributed generation sources and renewable energy sources can help curtail the present energy crisis and also help modernize the traditional grid [132-143]. While some technologies have already become cost-effective, many important technologies like PV, fuel cells, and storage technologies remain expensive without some sort of financial support.

The cost analysis can be divided into three categories: capital cost, operating cost and engineering cost.

Capital Costs—Total equipment and installation costs for the microgrid as incurred by the owner of the microgrid. Capital cost is broken down into two main categories, the cost of the power conversion electronics and other major equipment (e.g. switches) and the cost of the other materials needed to install the power systems.

Operating Costs—Present value of total variable cost (primarily energy use, but also including ancillary revenue streams, maintenance, etc.) for a powers system to serve an end use function.

Engineering Costs—Site-specific engineering costs to integrate the components of the microgrid with each other and the microgrid to the surrounding power systems. It is anticipated that microgrids will be installed in diverse environments that may require individualized design solutions.

We received data from Navigant Research and Homer and worked with these data to get the objective as mentioned previously. This paper provides an insight into what factors typically drive the cost of a microgrid project: location, size, components, storage, etc. This analysis relies on an Excel-based spreadsheet model developed by HOMER to analyze the costs and benefits of microgrids. The model evaluates the cost of microgrid based on the user's specification of project costs, the project's design and operating characteristics, and the facilities and services the project is designed to support. Of note, the model analyzes a discrete operating scenario specified by the user; it does not identify an optimal project designer operating strategy.

6.1.1 Histogram and Principal Component Analysis

Histogram analysis

Firstly the micorgrid is classified into three sections i.e. commercial microgrid, community microgrid and military microgrid. The $/MW of every type of microgrid is calculated, which is one of the factors that influence the cost of microgrids.

Fig. 6.2 is a Commercial Microgrid Histogram. A histogram is a graphical representation of the distribution of numerical data. It is an estimate of the probability distribution of a continuous variable.

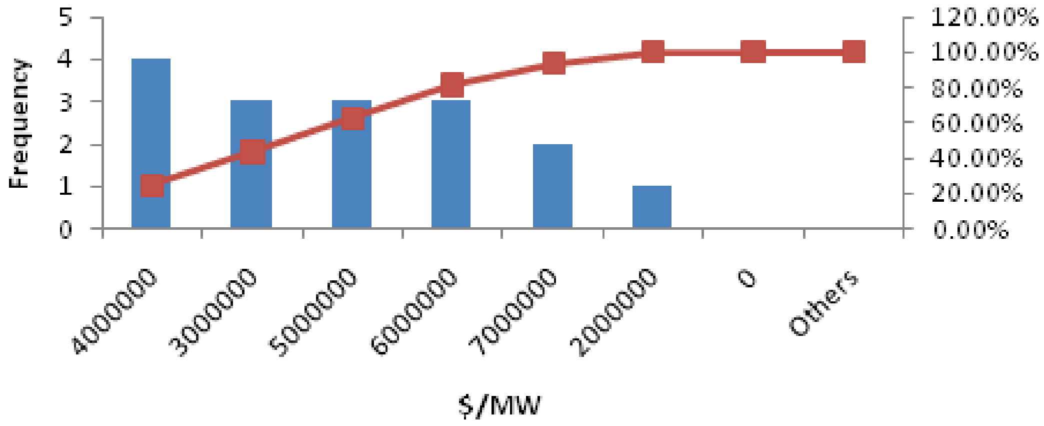

Fig. 6.2 Commercial Microgrid Histogram

A data point is included in a particular data set if the number is greater than the lowest bound and equal to or less than the largest bound for the data set. The highest frequency in this case is 4,000,000 $/MW. From the data, we can get some basic $/MW value on the commercial microgrid. The Min value is 1,083,109.92 $/MW, the Max Value is 6,395,348.837$/MW and the average value is 4,082,429.994$/MW.

Fig. 6.3 is a Community Microgrid Histogram. The highest frequency is 3,000,000 $/MW. From the data, we can get some basic $/MW value on the community microgrid. The Min value is 1,083,109.92 $/MW, the Max Value is 9,000,000 $/MW and the average value is 2,923,168.006 $/MW.

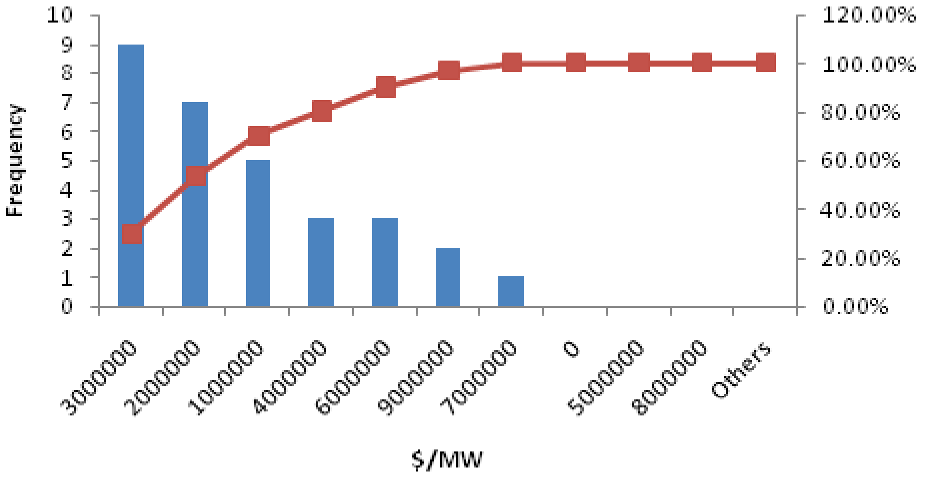

Fig. 6.3 Community Microgrid Histogram

Fig. 6.4 is a military microgrid histogram. The highest frequency is 4,000,000 $/MW. From the data, we can get some basic $/MW value on the military microgrid. The Min value is 848,636.3636$/MW, the Max Value is 48,026,699.39$/MW and the average value is 7,393,730.615$/MW.

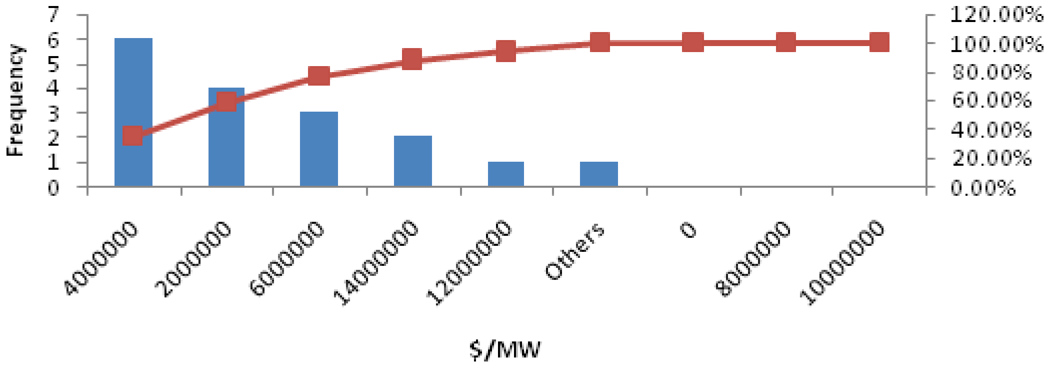

Fig. 6.4 Military Microgrid Histogram

Based on the above analysis, an estimate of the probability distribution of $/MW of various types of microgrid can be drawn.

Principal Component Analysis

The costs of microgrids are affected by many different factors. Factors including conventional generation capacity, renewable generation capacity, battery capacity and microgrid control cost contribute to costs of microgrid projects at different level. Therefore, it is necessary to employ PCA (principal component analysis) in order to identify major factors that determine the cost of microgrid.

Approaches of conducting PCA for microgrids' cost study can be listed as below:

- Obtain data from Navigant database and HOMER database;
- Subtract the mean value from observations;
- Calculate the covariance matrix;
- Calculate the eigenvectors and eigenvalues of the covariance matrix;
- Choosing major components and forming a feature vector;
- Deriving the new data set.

Fig. 6.5 gives preliminary results of PCA for generation capacity of micrgrids. In this case, capacities of different generation units which are diesel capacity, natural gas capacity, CHP (combined heat and power) capacity, PV capacity, wind capacity, energy storage capacity, energy storage duration and fuel cell capacity have been considered. Including microgrids' cost, initial data can be presented in a 9-dimensional dataset. By employing PCA, principal component can be identified, F1 in this case. Actually F1 is the linear combination of capacities of different generation units.

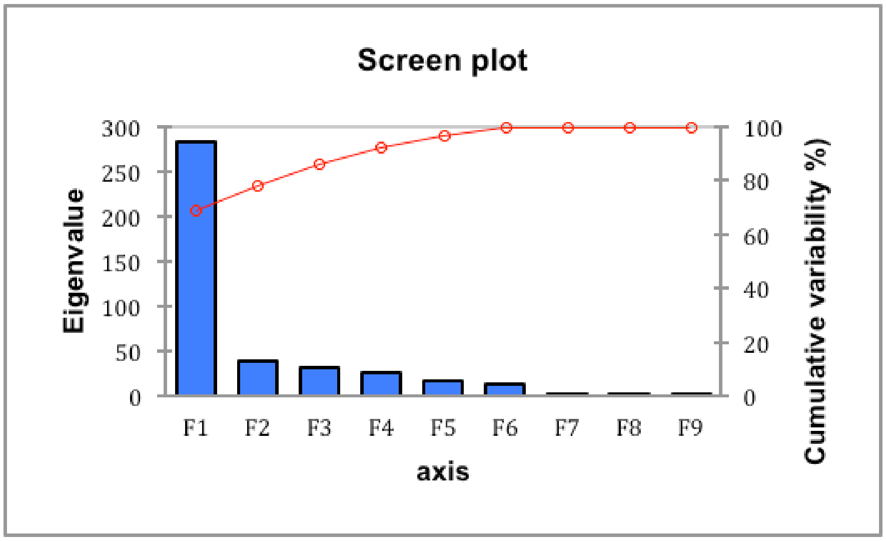

Fig. 6.5 PCA for generation capacity

Pertaining to PCA based on generation capacity, components F1, F2, F3, F4 and F5 can be chosen for further investigation. Eigenvalue of certain component represents its importance. Even though component F6 to F9 has been neglected, more than 96% of information can be retained. On the other hand, PCA has the capability of simplify dataset in microgrids' cost study.

According to Table XI, the capacity of CHP contributes 98.083% to component F1. The highest eigenvalue, eigenvalue corresponds to component F1, is the principal component of the dataset. Therefore, the major factor that affects the cost of microgrid project can be identified as the capacity of CHP.

Table 6.1 Contribution of the variables (%) towards generation capacity

	F1	F2	F3	F4	F5
Diesel Capacity	0.032	2.306	88.613	7.450	1.534
Natural Gas Capacity	1.768	94.567	1.276	1.491	0.515
CHP Capacity	98.083	1.839	0.006	0.021	0.005
PV Capacity	0.019	0.291	0.007	3.353	4.485
Wind Capacity	0.000	0.000	0.001	0.014	0.004
Energy Storage Capacity	0.003	0.010	0.004	0.092	1.555
Energy Storage Duration	0.023	0.093	1.016	0.704	91.161
Fuel Cell Capacity	0.000	0.001	0.001	0.001	0.005
Total Cost	0.070	0.893	9.077	86.875	0.736

It is important to notice that eigenvectors, which associates with eigenvalues obtained above, are perpendicular to each other. Then we can transform original dataset to new reference using eigenvectors as axis.

Fig. 6.6 shows the distribution of transformed dataset. Since we already determined that F1 is the principal component in this study, we select F1 as x-axis. The observations tend to distribute along the x-axis under new reference. Observations can also deviate from x-axis with the force conducted by y- axis component. If the force conducted by y-axis component, in this case which is component F2, becomes bigger, it drives observations further from x-axis.

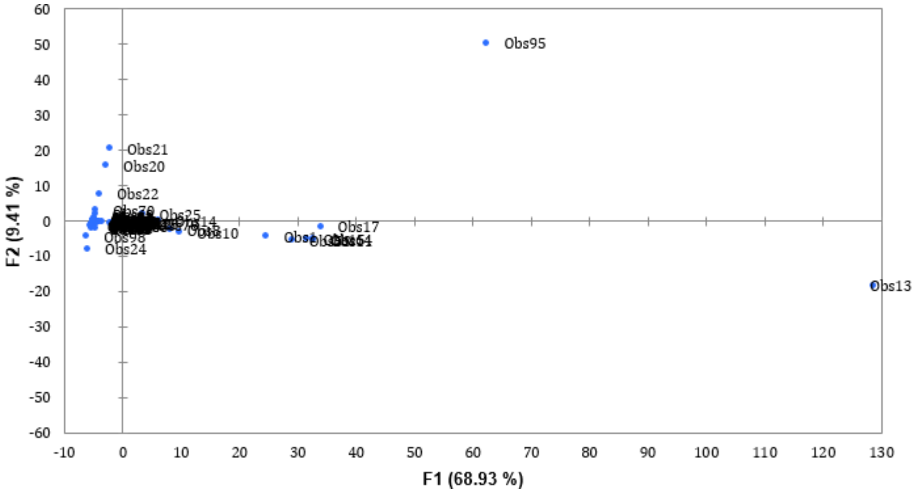

Fig. 6.6 Data distribution after reference transformation

In Fig. 6.6, clearly it can be seen that obs. 13 and obs. 95 are apart from main data group. Referring the original dataset, obs. 13 possesses 135MW CHP capacity and no other generation unit. Obs. 95 possesses 60MW natural gas capacity and no other generation unit.

Fig. 6.7 gives preliminary results of PCA for microgrids' generation categories. In this case, we divided generation units into 3 categories, which are conventional generation (diesel, CHP and natural gas), renewable generation (PV and wind generation), energy storage. Including microgrids' cost and number of generation source, initial data can be presented in a 5-dimensional dataset. By employing PCA, principal component can be identified.

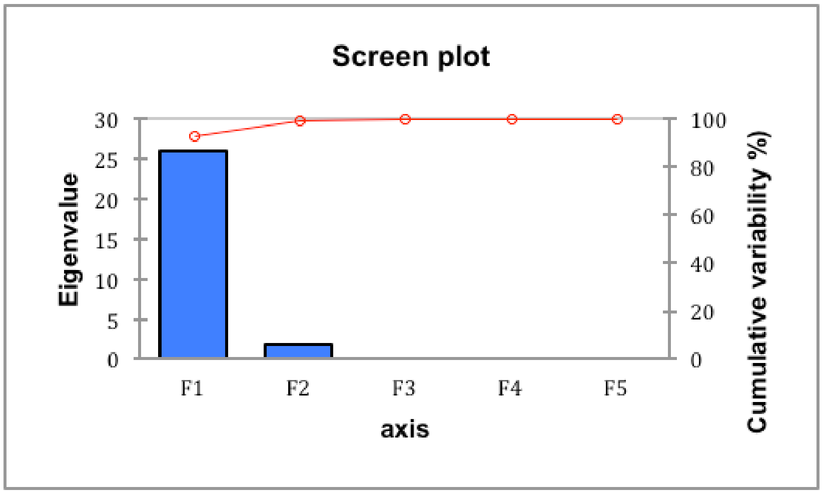

Fig. 6.7 PCA aims to generation categories

Fig. 6.8 shows the distribution of transformed dataset. Since Similarly, we select F1 as x-axis. As we can see, the observations tend to distribute along the x-axis. According to Fig. 70, we only have one outlier i.e. obs. 98. Besides, component F2 has very little effect on observation. Therefore, we have to search other information other than generation categories to investigate the cost of obs. 98. The relationship between microgrid total cost and generation categories cannot be demonstrated in this case since generation categories information have been neglected greatly during PCA.

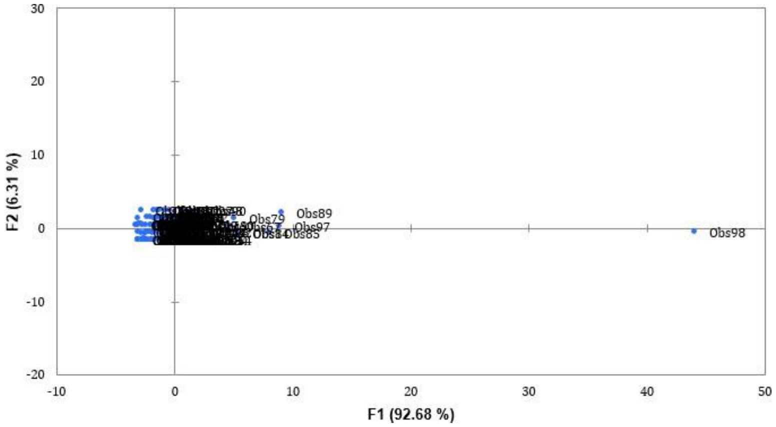

Fig. 6.8 Data distribution after reference transformation

With respect to PCA for generation categories, components F1 and F2 can be chosen to be further investigated. Even though components F3 to F5 have been neglected, more than 98% of information can be retained. According to Table XII, Total Cost contributes 99.888% to component F1. Hence component F1 is the principal component of the dataset. Therefore, Total Cost can be determined as principal component to affect data pattern.

Table 6.2 Contribution of the variables (%) that aims to generation categories

	F1	**F2**	**F3**	**F4**	**F5**
Percentage of Conventional Generation	0.036	0.860	72.383	0.030	26.691
Percentage of Renewable Generation	0.035	0.185	16.742	39.316	43.722
Percentage of Storage	0.000	0.166	9.609	60.640	29.585
Number of Sources	0.040	98.738	1.217	0.004	0.001
Total Cost	99.888	0.051	0.050	0.010	0.001

6.2 Discussions

From the Histogram analysis and Principal component analysis, it is evident that conventional sources (especially CHP) has an upper hand in determining the cost of the microgrids. Factors including conventional generation capacity, renewable generation capacity, battery capacity and microgrid control cost contribute to costs of microgrid projects as well.

Chapter 7. Research Conclusion and Future Work

7.1 Conclusion

This Consensus–based algorithm was used to analyze the behavior of microgrid during grid-connected mode. The microgrid shows good response during less and medium noise level. It brings the system close to its set point for incremental cost in less time. However, it was observed that it took longer for the system to reach its set point for noise levels higher than 0.8 level variance. The system oscillated around the set point value for a longer time and hence can be concluded that it was not stable to the desired level. Thus, this economic dispatch algorithm is very good for small and medium noises as it brings stability to the system in a short span of time based on the case study. The proposed consensus based algorithm for economic dispatch works well for islanded microgrids as well. In this dissertation, the consensus-based algorithm was used to analyze the behavior of microgrid during islanded mode in conjunction with STATCOM based reactive power compensation. The microgrid shows good response for different noise levels when reactive power is compensated in the system. It brings the system close to constant output power in less time. However, it was observed that it took longer for the system to reach its desired stability without any reactive power compensation. The system had more harmonics and oscillations for a longer time and hence can be said that it takes longer to achieve stability. It can be concluded from this study, that this consensus based economic dispatch algorithm with reactive power compensation is very good for islanded microgrids during small, medium, and large variance noises. It provides stability, efficiency, and resiliency to the system in a short span of time based on the case study.

With inclusion of VSG control strategy the system is able to stabilize much faster in the event of noise and load changes as seen from the results section. In islanded-mode of operation, the performance of VSG control strategy with STATCOM controller on voltage, frequency, active power, reactive power, are better than using only STACOM controller. These control strategies provide secondary and tertiary control of microgrid in grid-connected/islanded mode. Further control strategies may be introduced to provide for primary control.

7.2 Future research

Currently, the research has only focused on reactive power compensation in islanded microgrids. Further research will be aimed at using reactive power compensation with VSG for grid-connected Microgrid and its impact on Economic dispatch. More algorithms will be compared in grid-connected/islanded microgrids to get a better idea of economic dispatch for reactive power compensation. For future work, mixed integer programming will be analyzed to solve economic dispatch problem. More research work will be carried out to decrease response time, settling time, and overshoot. Frequency stabilizing time will also be improved. Effect of large variance noise will be reduced further to make the microgrids more stable and efficient.

List of Publications

Published:

Shruti Singh, David Wenzhong Gao, Julieta Giraldez, “Cost Analysis of Renewable Energy-based Microgrids,” in *2017 North American Power Symposium (NAPS)*, 2017, pp. 1–5.

Shruti Singh, David Wenzhong Gao, “Noiseless Consensus based Algorithm for Economic Dispatch problem in Grid-connected Microgrids to enhance Stability among Distributed Generators,” in *2019 North American Power Symposium (NAPS)*, 2019, pp. 1–6.

Shruti Singh, David Wenzhong Gao, “Noiseless Consensus based Economic Dispatch Algorithm in conjunction with STATCOM Controller for Reactive Power Compensation in Islanded Microgrids to enhance Voltage and Power Stability,” in *2019 North American Power Symposium (NAPS)*, 2019, pp. 1–7.

Shruti Singh and David Wenzhong Gao,“Improved Virtual Synchronous Generator principle for better Economic Dispatch and stability in Grid-connected Microgrids with low noise,” in *Energies*, vol.16, no. 12, 2023.

Shruti Singh and David Wenzhong Gao,“ Comparison amongst Lagrange, Firefly, and ABC Algorithms for better low noise Economic Dispatch and Reactive Power Compensation in Islanded Microgrids,” in *Energies,* **Accepted for publication**

References

[1] D. Liu, Y. Cai, “Taguchi method for solving the economic dispatch problem with nonsmooth cost functions”, IEEE Trans. Power Syst., vol. 20, no. 4, pp. 2006–2014, Nov. 2005.

[2] J. B. Park, Y. W. Jeong, J. R. Shin, K. Lee, “An improved particle swarm optimization for nonconvex economic dispatch problems”, IEEE Trans. Power Syst., vol. 25, no. 1, pp. 156–166, Feb. 2010.

[3] T. Guo, M. Henwood, M. Van Ooijen, “An algorithm for combined heat and power economic dispatch”, IEEE Trans. Power Syst., vol. 11, no. 4, pp. 1778–1784, Nov. 1996.

[4] J. Y. Fan, L. Zhang, “Real time economic dispatch with line flow and emission constraints using quadratic programming”, IEEE Trans. Power Syst., vol. 13, no. 2, pp. 320–325, May 1998.

[5] Jordehi, Javadi, Catalao, “Dynamic Economic Load Dispatch in Isolated Microgrids with Particle Swarm Optimisation considering Demand Response,” 55th International Universities Power Engineering Conference (UPEC), pp. 1-5, 2020.

[6] Imtiaz, Cui, Zafar, “Economic Dispatch of Microgrid incorporating Demand Response using Dragonfly Algorithm,” IEEE International Conference on Advances in Electrical Engineering and Computer Applications (AEECA), pp. 59-68, 2021.

[7] Singh, Poddar, Ramalingam, Shanmugam, Kalam, “Investigation on Dynamic Economic Dispatch Problem of Microgrid using Cuckoo Search Algorithm – Grid connected and Island mode,” IEEE Region 10 Conference (TENCON), pp. 1886-1891, 2019.

[8] Ning Luo, Jinsen Liu, and Pengcheng Zhang, “Optimal Dispatching of Active Distribution Network based on Improved Genetic Algorithm,” 44th International Conference on Frontiers Technology of Information and Computer (ICFTIC), pp. 551-554, 2022.

[9] T. K. Panigrahi, A. K. Sahoo, and A. Behera, “A review on application of various heuristic techniques to combined economic and emission dispatch in a modern power system scenario,” *Energy Procedia*, vol. 13, pp. 458–463, Oct. 2017.

[10] A. N. Afandi, “Optimal scheduling power generations using HSABC algorithm considered a new penalty factor approach,” 2nd IEEE Conference on Power Engineering and Renewable Energy (ICPERE), pp. 13–18, 2014.

[11] Y. Shang, S. Lu, J. Gong, R. Liu, X. Li, and Q. Fan, “Improved genetic algorithm for economic load dispatch in hydropower plants and comprehensive performance comparison with dynamic programming method,” *J. Hydrol.*, vol. 554, no. Supplement C, pp. 306–316, Nov 2017.

[12] A. N. Afandi, “Solving Combined Economic and Emission Dispatch Using Harvest Season Artificial Bee Colony Algorithm Considering Food Source Placements and Modified Rates,” Int. J. Electr. Eng. Inform., vol. Vol. 6, p. 267, Jul 2014.

[13] A. N. Afandi, I. Fadlika, and A. Andoko, “Comparing Performances of Evolutionary Algorithms on the Emission Dispatch and Economic Dispatch Problem,” TELKOMNIKA Telecommun. Comput. Electron. *Control*, vol. 13, no. 4, pp. 1187–1193, Dec. 2015.

[14] R. Olfati-Saber, R. M. Murray, “Consensus problems in networks of agents with switching topology and time-dalys”, IEEE Trans. Autom. Control, vol. 49, no. 9, pp. 1520-1533, 2004.

[15] W. Ren, R. W. Beard, E. M. Atkins, “Information consensus in multivehicle cooperative control”, IEEE Control Syst. Mag., pp. 71-82, Apr. 2007.

[16] A. Jadbabaie, J. Lin, A. S. Morse, “Coordination of groups of mobile autonomous agents using nearest neighbor rules”, IEEE Trans. Autom. Control, vol. 50, no. 2, pp. 169-182, 2005.

[17] L. Moreau, “Stability of multiagent systems with time-dependent communication links”, IEEE Trans. Autom. Control, vol. 50, no. 2, pp. 169-182, 2005.

[18] Ma, Zhang, Liu, Yang, “Fully distributed social welfare optimization with line flow constraint consideration”, IEEE Trans. Ind. Informat, vol. 11, no. 6, pp. 1532-1540, 2015.

[19] Rahbari, Ojha, Zhang, Chow, “Incremental welfare consensus algorithm for cooperative distributed generation/demand response in smart grid”, IEEE Trans. Smart Grid, vol. 5, no. 6, pp. 2836-2845, 2014.

[20] Xu, Li, “Distributed optimal resource management based on consensus algorithm in a microgrid”, IEEE Trans. Ind. Electron, vol. 62, no. 4, pp. 2584-2592, 2015.

[21] Xu, Yang, Gu, Li, Deng, “Robust real-time distributed optimal control based energy management in a smart grid”, IEEE Trans. Smart Grid, vol. 8, no. 4, pp. 1568-1579, 2017.

[22] Zheng, Wu, Zhang, Lin, “Distributed optimal residential demand response considering operational constraints of unbalanced distribution networks”, IET Generation, Transmission & Distribution, vol. 12, no. 9, pp. 1970-1979, 2018.

[23] Guo, Wen, Li, “Distributed optimal energy scheduling based on a novel PD pricing strategy in smart grid”, IET Generation, Transmission & Distribution, vol. 11, no. 8, pp. 2075-2084, 2017.

[24] Rahbari, Zhang, Chow, “Consensus-based distributed scheduling for cooperative operation of distributed energy resources and storage devices in smart grids”, IET Generation, Transmission & Distribution, vol. 10, no. 5, pp. 1268-1277, 2016.

[25] Abhinav, Schizas, Lewis, Davoudi, “Distributed noise-resilient networked synchrony of active distribution systems”, IEEE Trans. Smart Grid, vol. 9, no. 2, pp. 836-846, 2018.

[26] Abhinav, Schizas, Ferrese, Davoudi, “Optimization based Ac microgrid synchronization”, IEEE Trans. Ind. Informat, vol. 13, no. 5, pp. 2339-2349, 2017.

[27] Dehkordi, Baghaee, Sadati, Guerrero, “Distributed noise-resilient secondary voltage and frequency control for islanded microgrids”, IEEE Trans. Smart Grid, 2018, DOI: 10.1109/TSG.2018.2834951.

[28] F. Chen, M. Chen, Zhao, Guerrero, Wang, “Distributed Noise-resilient economic dispatch strategy for islanded microgrids”, IET Generation, Transmission & Distribution, May 2019, DOI: 10.1049/iet-gtd.2018.5740.

[29] Yazdanian, Mehrizi, Sani, “Distributed control techniques in microgrids”, IEEE Trans. Smart Grid, vol. 5, no. 6, pp. 2901-2909, 2014.

[30] Molzahn, Dorfler, Sandberg, Low, Chakrabarti, Baldick, et. al., “A survey of distributed optimization and control algorithms for electric power systems”, IEEE Trans. Smart Grid, vol. 8, no. 6, pp. 2941-2962, 2017.

[31] Han, Zhang, Li, Coelho, Guerrero, “MAS-based distributed coordinated control and optimization in kicrogrid and microgrid clusters: A comprehensive review”, IEEE Trans. Power Electron, vol. 33, no. 8, pp. 6488-6508, 2018.

[32] Xu, Wu, Sun, Wang, “Fully distributed multi-area dynamic economicdispatch method with second-order convergence for active distribution networks”, IET Generation, Transmission & Distribution, vol. 11, no. 16, pp. 3955-3965, 2017.

[33] Lysikatos, Hatziargyriou, “Fully distributed economic dispatch of distributed generators in active distribution networks considering losses”, IET Generation, Transmission & Distribution, vol. 11, no. 3, pp. 627-636, 2017.

[34] Zheng, Wu, Zhang, Li, Liu, “Fully distributed multi-area economic dispatch method for active distribution networks”, IET Generation, Transmission & Distribution, vol. 9, no. 12, pp. 1341-1351, 2015.

[35] Y. Tu, J. H. Su, Y. Du, X. Z. Yang, H. D. Xu, “Analysis of microgrid inverter paralleling system based on virtual oscillator,” Electric Power Automation Equipment, vol. 37, no. 9, pp. 24-30, 2017.

[36] Q. M. Cheng, J. Gao, Y. M. Cheng, “An inverter control method suitable for islanding operation,” Power System Technology, vol. 42, no. 1, pp. 203-209, 2018.

[37] Y. Q. Xu, H. J. Ma, “Inverter parallel operation technology based on improved droop control,” Power System Protection and Control, vol. 43, no. 7, pp. 103-107, 2015.

[38] Z. Y. Lü, Z. J. Wu, X. B. Dou, “Adaptive discrete droop control of isolated DC microgrid based on discrete consistency,” Proceedings of the CSEE, vol. 35, no. 17, pp. 4397-4407, 2015.

[39] J. Meng, X. Shi, Y. Wang, “A virtual synchronous generator control strategy for distributed generation,” Electricity Distribution (CICED), 2014 China International Conference on. IEEE, pp. 495-498.

[40] Bansal, “Three phase self excited induction generators: An overview”, IEEE Transaction on energy conversion, vol. 20, no. 2, pp. 292-299, 2005.

[41] Dong Lee, Wang Li, “Small signal stability analysis of an autonomous hybrid renewable energy power generation/energy storage system time domain simulations”, IEEE Transaction for Energy Conversion, vol. 23, no. 1, pp. 311-320, 2008.

[42] Murty, Malik, Tondon, “Analysis of self excited induction generator”, IEEE Proceedings C – Generation, Transmission and Distribution, vol. 129, no. 6, pp. 260-265, 1982.

[43] Feng Wei, Sun Kai, Guan Yajuan, Wang Yibo, “A Harmonic Current Suppression Strategy for Voltage Source Grid-Connected Inverters Based on Output Voltage Hybrid Control in Islanded Microgrids”, Transactions of China electrotechnical society, vol. 31, no.7, pp. 72-80, 2016.

[44] Guerrero J M , et al, “Hierarchical control of droop-controlled AC and DC microgrids a general approach toward standardization”, IEEE Transactions on Industrial Electronics, vol. 58, no.1, pp. 158-172, 2011.

[45] Qin Wenping, Liu Xuesong, Han Xiaoqing, “An Improved Control Strategy of Automatic Charging/Discharging of Energy Storage System in DC Microgrid”, vol. 38, no. 7, pp. 1827-1834, 2014.

[46] Dang Ke, Hu Jin, Yan Gan-gui, “Research on Low Voltage Ride through Control Strategy of Photovoltaic Inverter”, Power Electronics, vol. 47, no. 11, pp. 22-24, 2013.

[47] Chen Xin,Wei Zheng, Hu Xuefeng,Cen Yihan, Gong Chunying, “Research on LCL Filter in Three-Phase Grid-Connected Inverter and Novel Active Damping

Control Strategy", Transactions of China Electrotechnical Society, vol. 29, no. 6, pp. 71-79, 2014.

[48] Shenghai Zhou, Ying Gu, Wei Song, Chong Wang, Feng Bai, Yong Cai, "Research on Control Strategy of Grid-Connected Inverter in Microgrid System", Preprints of the 3rd IEEE conference on Energy Internet and Energy System Integration, 2019.

[49] Moayedi, S.; Davoudi, A., "Distributed Tertiary Control of DC Microgrid Clusters," IEEE Transactions on Power Electronics , vol.31, no.2, pp.1717-1733, Feb. 2016

[50] Guerrero, J.M, Vasquez J.C, Matas J, de Vicuña L.G, Castilla M., "Hierarchical Control of Droop-Controlled AC and DC Microgrids—A General Approach Toward Standardization," IEEE Transactions on Industrial Electronics, vol.58, no.1, pp.158-172, Jan. 2011.

[51] Dan Wu, Fen Tang, Tomislav Dragicevic, Josep M. Guerrero, Juan C. Vasquez, "Coordinated Control Based on Bus-Signaling and Virtual Inertia for DC Islanded Microgrids," IEEE Transactions on Smart Grid, vol.6, no.6, pp. 2627-2638, 2015.

[52] C. N. Papadimitriou, E. I. Zountouridou and N. D. Hatziargyriou, "Review of hierarchical control in DC microgrids," Electric Power Systems Research, vol. 122, pp. 159-167, 2015.

[53] C. Jin, P. Wang, J. Xiao, Y. Tang, and F. H. Choo, "Implementation of hierarchical control in dc microgrids," IEEE Trans. Ind. Electron., vol. 61, no. 8, pp. 4032–4042, Aug. 2014.

[54] J. Schonberger, R. Duke, and S. D. Round, "DC-bus signaling: A distributed control strategy for a hybrid renewable nanogrid," IEEE Trans. Ind. Electron., vol. 53, no. 5, pp. 1453–1460, Oct. 2006.

[55] C. Yin, H. Wu, F. Locment, and M. Sechilariu, "Energy management of dc microgrid based on photovoltaic combined with diesel generator and supercapacitor," Energy Conversion Management, vol. 132, pp. 14–27, Jan. 2017.

[56] A. Tani, M. Camara, and B. Dakyo, “Energy management in the decentralized generation systems based on renewable energy ultracapacitors and battery to compensate the wind/load power fluctuations,” IEEE Trans. Ind. Appl., vol. 51, no. 2, pp. 1817–1827, Mar./Apr. 2015.

[57] M. A. Tankari, M. B. Camara, B. Dakyo, and G. Lefebvre, “Use of ultracapacitors and batteries for efficient energy management in winddiesel hybrid system,” IEEE Trans. Sustain. Energy, vol. 4, no. 2, pp. 414–424, Apr. 2013.

[58] D. Chandran, M. Joshi, and V. Agarwal, “Solar PV based retrofit solution for cell phone towers powered by diesel generators,” in Proc. IEEE Int. Telecommun. Energy Conf., pp. 1–8, 2016.

[59] Y. Gu, X. Xiang, W. Li, and X. He, “Mode-adaptive decentralized control for renewable dc microgrid with enhanced reliability and flexibility,” IEEE Trans. Power Electron., vol. 29, no. 9, pp. 5072–5080, Sep. 2014.

[60] T. Morstyn, B. Hredzak, G. Demetriades, and V. Agelidis, “Unified distributed control for DC microgrid operating modes,” IEEE Trans. Power Syst., vol. 31, no. 1, pp. 802–812, Jan. 2015.

[61] P. Sanjeev, N. Padhy, and P. Agarwal, “Peak energy management using renewable integrated dc microgrid,” IEEE Trans. Smart Grid, vol. 9, no. 5, pp. 4906–4917, Sep. 2018.

[62] B. Dong, L. Yongdong, and Z. Zhixue, “Control strategies of dc-bus voltage in islanded operation of microgrid,” in Proceedings of 4th International Conference Electric Utility Deregulation Restructing Power Technology, pp. 1671–1674, 2011.

[63] N. Eghtedarpour and E. Farjah, “Power control and management in a hybrid AC/DC microgrid,” IEEE Trans. Smart Grid, vol. 5, no. 3, pp. 1494–1505, Apr. 2014.

[64] R. Majumder, “A hybrid microgrid with DC connection at back to back converters,” IEEE Trans. Smart Grid, vol. 5, no. 1, pp. 251–259, Jun. 2014.

[65] M. Hosseinzadeh and F. R. Salmasi, “Power management of an isolated hybrid AC/DC micro-grid with fuzzy control of battery banks,” IET Renewable Power Gener., vol. 9, no. 5, pp. 484–493, Jun. 2015.

[66] F. Katiraei, M. R. Iravani, P. W. Lehn, “Micro-Grid Autonomous Operation During and Subsequent to Islanding Process,” IEEE Trans. Power Delivery, vol. 20, no. 1, pp.248-257, Jan. 2005.

[67] T G Yang, W H Gui, “Research on a particle swarm optimization adaptive backstepping control method of grid-connected inverters”, Proceedings of the CSEE, vol. 36, no. 11, 3036-3044, 2016.

[68] X Q Shen, H Q Wang, “Distributed secondary voltage control of islanded microgrids based on RBF-neural network sliding-mode technique”, IEEE Access, vol. 29, no. 15, pp. 5-9, 2019.

[69] H Teimour, K Hamed, “Decentralised robust T-S fuzzy controller for a parallel islanded AC microgrid”, IET Generation Transmission & Distribution, vol. 18, no. 4, pp. 5-7, 2019.

[70] Z W Li, C Z Zang, P Zeng, et al, “Control of a gridforming inverter based on sliding mode and mixed H2/H∞ control”, IEEE Transactions on Industrial Electronics, vol. 64, no. 5, pp. 3862-3866, 2016.

[71] M C Pulcherio, M S Illindala, R K Yedavalli, “Robust stability region of a microgrid under parametric uncertainty using Bialternate sum matrix approach”, IEEE Transactions on Power Systems, vol. 33, no. 5, pp. 5553-5559, 2018.

[72] L Chen, H Nian, Y Y Xu, “Improved model predictive direct power control of grid side converter in weak grid using Kalman filter and DSOGI”, Chinese Journal of Electrical Engineering, vol. 5, no. 4, pp 22-32, 2019.

[73] A Tavakoli, M Negnevitsky, K Muttaqi, “A decentralized model predictive control for operation of multiple distributed generators in islanded mode”, IEEE Transactions on Industry Applications, vol. 5, no. 2, pp. 1466-1475, 2017.

[74] Z Y Chen, A Luo, H J Wang, et al, “Adaptive sliding-mode voltage control for inverter operating in islanded mode in microgrid”, International Journal of Electrical Power & Energy Systems, vol. 6, no. 6, pp. 133-143, 2015.

[75] R Gupta, S K Gudey, “Recursive fast terminal sliding mode control in voltage source inverter for a low-voltage microgrid system”, IET Generation, Transmission & Distribution, vol. 10, no. 7, pp. 1536-1543, 2016.

[76] M M Zhang, Y Li, F Liu, et al., “Cooperative operation of DG inverters and a RIHAF for power quality improvement in an integrated transformer-structured grid-connected microgrid”, IEEE Transactions on Industry Applications, vol. 55, no. 2, pp. 1157-1170, 2019.

[77] H Li, Y Li, J M Guerrero, et al., “A comprehensive inertial control strategy for hybrid AC/DC microgrid with distributed generations”, IEEE Transactions on Smart Grid, vol. 11, no. 2, pp. 1737-1747, 2020.

[78] Y Wang, Z Chen, X Wang, et al., “ An estimator-based distributed voltage-predictive control strategy for AC islanded microgrids”, IEEE Transactions on Power Electronics, vol. 30, no. 7, pp. 3934-3951, 2015.

[79] B Abdeldjabar, X Dianguo, G Zhiqiang, “Active disturbance rejection control of LCL filtered grid connected inverter using padé approximation”, IEEE Transactions on Industry Applications, vol. 54, no. 6, pp. 6179- 6186, 2018.

[80] Amir Enayati, Thomas H. Ortmeyer, “Peak load carying capability of a resilient microgrid in islanded mode”, IEEE Power & Energy Society Innovative Smart Grid Technologies Conference (ISGT), 2016.

[81] Kumar J, Agarwal A, Agarwal V, “A review on overall control of DC microgrids”, Journal of Energy Storage, vol. 21, pp.113-138, 2019.

[82] M. Saleh, Y. Esa and A. A. Mohamed, “Communication-Based Control for DC Microgrids”, IEEE Transactions on Smart Grid, vol. 10, no. 2, pp. 2180-2195, March 2019.

[83] Zhu Shanshan, Wang Fei, Guo Hui, et al. “Overview of Droop Control in DC Microgrid”, Proceeding of the CSEE, vol. 3, no. 1, pp. 72-84, 2018.

[84] Wenguang Zhao, Xing Zhang, Yanjun Li, Nixin Qian, “Improved master-slave control for Smooth Transition Between Grid-connected and Islanded Operation of DC Microgrid Based on I -ΔV Droop”, IEEE 9th International Power Electronics and Motion Control Conference (IPEMC2020-ECCE Asia), 2020.

[85] H. Reduan and J. Khyan, “A Comprehensive Review of the Application Characteristics and Traffic Requirements of a Smart Grid Communications Network”, Computer Networks, vol. 57, no. 3, pp. 825- 845, 2013.

[86] J. O. Dada, “Towards understanding the benefits and challenges of Smart/Micro-Grid for electricity supply system in Nigeria”, Renewable and Sustainable Energy Reviews, vol. 38, p. 1003–1014, 2014.

[87] N. Lidula and A. Rajapakse, “Microgrids Research: A Review of Experimental Microgrids and Test System”, Renewable and Sustainable Energy Reviews, vol. 15, no. 1, pp. 186-202, 2011.

[88] E. Ancillotti, R. Bruno and Conti.M., “The role of communication system in smart grids: Architectures, technical solutions and research challengues”, Computer Communications, vol. 36, no. 17, pp. 1665- 1697, 2013.

[89] V. Gungor, D. Sahin, T. Kocak, S. Ergut, C. Buccella, C. Cecati and G. Hancke, “A survey on smart grid potential applications and communication requirements”, IEEE Trans. on Industrial Informatics,vol. 9, no. 1, pp. 28-42, 2013.

[90] O. Palizban, K. Kauhaniemi and J. M. Guerrero, “Microgrids in Active Network Management – Part II: System Operation, Power Quality and Protection”, Renewable and Sustainable Energy Reviews, vol. 36, pp. 440-441, 2014.

[91] R. Deng, Z. Yang, M. Y. Chow and J. Chen, “A survey on demand response in smart grids: Mathematical models and approaches”, IEEE Trans. on Industrial Informatics, vol. 11, no. 3, pp. 570-582, 2015.

[92] X. Yi and P.Wang, “Security Framework for Wireless Communications in Smart Distribution Grid”, IEEE Trans. on Smart Grid, vol. 2, no. 4, pp. 809-818, 2011.

[93] R. Prior, D. E. Lucani, Y. Phulpin, M. Nistor and J. Barros, “Network Coding Protocols for Smart Grid Communications”, IEEE Trans. on Smart Grid, vol. 5, no. 3, pp. 1523-1531, 2014.

[94] A. K. M. Baki, “Continuous Monitoring of Smart Grid Devices Through Multi Protocol Label Switching”, IEEE Trans. on Smart Grid, vol. 5, no. 3, pp. 1210-1215, 2014.

[95] E. Padilla, K. Agbossou and A. Cardenas, “Towards Smart Integration of Distributed Energy Resources Using Distributed Network Protocol Over Ethernet”, IEEE Trans. on Smart Grid, vol. 5, no. 4, pp. 1686- 1695, 2014.

[96] C. Zhao, J. He, P. Cheng and J. Chen, “Consensus-Based Energy Management in Smart Grid With Transmission Losses and Directed Communication”, IEEE Transactions on Smart Grid, no. 99, pp. 1-13, 2016.

[97] C. H. Lo and N. Ansari, “Decentralized Controls and Communications for Autonomous Distribution Networks in Smart Grid”, IEEE Trans. on Smart Grid, vol. 4, no. 1, pp. 66-77, 2013.

[98] A. Lopes and Botelho.L, “Improving Multi-Agent Based Resource Coordination in Peer-to-Peer Networks”, Journal of Networks, vol. 3, no. 2, 2008.

[99] C. Giotitsas, A. Pazaitis and V. Kostakis, “A peer-to-peer approach to energy production”, Technology in Society, vol. 42, pp. 28-38, 2015.

[100] M. Amoretti, “The peer-to-peer paradigm applied to hydrogen energy distribution”, EUROCON 2009, IEEE, pp. 494-500, 2009.

[101] H. D. Bandara and A. P. Jayasumana, “Collaborative applications over peer-to-peer systems–challenges and solutions”, Peer-to-Peer Networking and Applications, vol. 6, no. 3, pp. 257-276, 2013.

[102] F. Chen, M. Chen, Zhao, Guerrero, Wang, “Distributed Noise-resilient economic dispatch strategy for islanded microgrids”, IET Generation, Transmission & Distribution, May 2019, DOI: 10.1049/iet-gtd.2018.5740.

[103] Abhinav, Schizas, Lewis, Davoudi, “Distributed noise-resilient networked synchrony of active distribution systems”, IEEE Trans. Smart Grid, vol. 9, no. 2, pp. 836-846, 2018.

[104] Hua Li, Rui-Zheng Gu, “Research on Grid-coonected Control and Simulation of Microgrid Inverter based on VSG”, China International Conference on Electricity Distribution, Tianjin, Sep. 2018.

[105] L. Moreau, “Stability of multiagent systems with time-dependent communication links”, IEEE Trans. Autom. Control, vol. 50, no. 2, pp. 169-182, 2005.

[106] D. Liu, Y. Cai, “Taguchi method for solving the economic dispatch problem with nonsmooth cost functions”, IEEE Trans. Power Syst., vol. 20, no. 4, pp. 2006–2014, Nov. 2005.

[107] J. B. Park, Y. W. Jeong, J. R. Shin, K. Lee, “An improved particle swarm optimization for nonconvex economic dispatch problems”, IEEE Trans. Power Syst., vol. 25, no. 1, pp. 156–166, Feb. 2010.

[108] T. Guo, M. Henwood, M. Van Ooijen, “An algorithm for combined heat and power economic dispatch”, IEEE Trans. Power Syst., vol. 11, no. 4, pp. 1778–1784, Nov. 1996.

[109] J. Y. Fan, L. Zhang, “Real time economic dispatch with line flow and emission constraints using quadratic programming”, IEEE Trans. Power Syst., vol. 13, no. 2, pp. 320–325, May 1998.

[110] R. Olfati-Saber, R. M. Murray, “Consensus problems in networks of agents with switching topology and time-delays”, IEEE Trans. Autom. Control, vol. 49, no. 9, pp. 1520-1533, 2004.

[111] W. Ren, R. W. Beard, E. M. Atkins, “Information consensus in multivehicle cooperative control”, IEEE Control Syst. Mag., pp. 71-82, Apr. 2007.

[112] A. Jadbabaie, J. Lin, A. S. Morse, “Coordination of groups of mobile autonomous agents using nearest neighbor rules”, IEEE Trans. Autom. Control, vol. 50, no. 2, pp. 169-182, 2005.

[113] L. Moreau, “Stability of multiagent systems with time-dependent communication links”, IEEE Trans. Autom. Control, vol. 50, no. 2, pp. 169-182, 2005.

[114] Ma, Zhang, Liu, Yang, “Fully distributed social welfare optimization with line flow constraint consideration”, IEEE Trans. Ind. Informat, vol. 11, no. 6, pp. 1532-1540, 2015.

[115] Rahbari, Ojha, Zhang, Chow, “Incremental welfare consensus algorithm for cooperative distributed generation/demand response in smart grid”, IEEE Trans. Smart Grid, vol. 5, no. 6, pp. 2836-2845, 2014.

[116] Xu, Li, “Distributed optimal resource management based on consensus algorithm in a microgrid”, IEEE Trans. Ind. Electron, vol. 62, no. 4, pp. 2584-2592, 2015.

[117] Xu, Yang, Gu, Li, Deng, "Robust real-time distributed optimal control based energy management in a smart grid", IEEE Trans. Smart Grid, vol. 8, no. 4, pp. 1568-1579, 2017.

[118] Zheng, Wu, Zhang, Lin, "Distributed optimal residential demand response considering operational constraints of unbalanced distribution networks", IET Generation, Transmission & Distribution, vol. 12, no. 9, pp. 1970-1979, 2018.

[119] Guo, Wen, Li, "Distributed optimal energy scheduling based on a novel PD pricing strategy in smart grid", IET Generation, Transmission & Distribution, vol. 11, no. 8, pp. 2075-2084, 2017.

[120] Rahbari, Zhang, Chow, "Consensus-based distributed scheduling for cooperative operation of distributed energy resources and storage devices in smart grids", IET Generation, Transmission & Distribution, vol. 10, no. 5, pp. 1268-1277, 2016.

[121] Abhinav, Schizas, Lewis, Davoudi, "Distributed noise-resilient networked synchrony of active distribution systems", IEEE Trans. Smart Grid, vol. 9, no. 2, pp. 836-846, 2018.

[122] Abhinav, Schizas, Ferrese, Davoudi, "Optimization based Ac microgrid synchronization", IEEE Trans. Ind. Informat, vol. 13, no. 5, pp. 2339-2349, 2017.

[123] Dehkordi, Baghaee, Sadati, Guerrero, "Distributed noise-resilient secondary voltage and frequency control for islanded microgrids", IEEE Trans. Smart Grid, 2018, DOI: 10.1109/TSG.2018.2834951.

[124] F. Chen, M. Chen, Zhao, Guerrero, Wang, "Distributed Noise-resilient economic dispatch strategy for islanded microgrids", IET Generation, Transmission & Distribution, May 2019, DOI: 10.1049/iet-gtd.2018.5740.

[125] Yazdanian, Mehrizi, Sani, "Distributed control techniques in microgrids", IEEE Trans. Smart Grid, vol. 5, no. 6, pp. 2901-2909, 2014.

[126] Molzahn, Dorfler, Sandberg, Low, Chakrabarti, Baldick, et al., "A survey of distributed optimization and control algorithms for electric power systems", IEEE Trans. Smart Grid, vol. 8, no. 6, pp. 2941-2962, 2017.

[127] Han, Zhang, Li, Coelho, Guerrero, "MAS-based distributed coordinated control and optimization in kicrogrid and microgrid clusters: A comprehensive review", IEEE Trans. Power Electron, vol. 33, no. 8, pp. 6488-6508, 2018.

[128] Xu, Wu, Sun, Wang, "Fully distributed multi-area dynamic economicdispatch method with second-order convergence for active distribution networks", IET Generation, Transmission & Distribution, vol. 11, no. 16, pp. 3955-3965, 2017.

[129] Lysikatos, Hatziargyriou, "Fully distributed economic dispatch of distributed generators in active distribution networks considering losses", IET Generation, Transmission & Distribution, vol. 11, no. 3, pp. 627-636, 2017.

[130] Zheng, Wu, Zhang, Li, Liu, "Fully distributed multi-area economic dispatch method for active distribution networks", IET Generation, Transmission & Distribution, vol. 9, no. 12, pp. 1341-1351, 2015.

[131] Bansal, "Three phase self excited induction generators: An overview", IEEE Transaction on energy conversion, vol. 20, no. 2, pp. 292-299, 2005.

[132] Dong Lee, Wang Li, "Small signal stability analysis of an autonomous hybrid renewable energy power generation/energy storage system time domain simulations", IEEE Transaction for Energy Conversion, vol. 23, no. 1, pp. 311-320, 2008.

[133] Murty, Malik, Tondon, "Analysis of self-excited induction generator", IEEE Proceedings C – Generation, Transmission and Distribution, vol. 129, no. 6, pp. 260-265, 1982.

[134] Padiyar, "FACTS controlling in power transmission system and distribution", New Age International Publishers, 2007.

[135] Mohanty, Viswavandya, Mishra, et al., "An optimized STATCOM controller for voltage stability and reactive power compensation in an isolated microgrid", IEEE Power, Communication and Information TechnologyConference, 2015.

[136] R. H. Lasseter, A. Akhil, C. Marnay, J. Stephens, J. Dagle, R. Guttromson, A. Meliopoulous, R. Yinger, and J. Eto, The CERTS microgrid concept, white paper on integration of distributed energy resources, U.S. Dept. Energy, California Energy Comm., Office of Power TechnolLBNL 50829, Apr. 2002. [Online].

Available: http://certs.lbl.gov

[137] A.Engler, O.Osika,M.Barnes, N.Jenkins,and A.Arulampalam, DB1 local micro source controller strategies and algorithms, Eur. Comm., Feb. 2004. [Online]. Available: www.microgrids.eu/micro2000

[138] Lee Kyebyung, Son KM, Gilsoo Jang, “Smart storage system for seamless transition of customers with intermittent renewable energy sources into microgrid”, 31st International telecommunications energy conference, pp. 1–5, 2009.

[139] Asmus Peter, “Microgrids distributed energy systems for campus, military, remote, community, and commercial & industrial power applications: market analysis and forecasts”, Pike Report, 2012.

[140] Sofla Mohammadhassan Abdollahi, Gharehpetian Gevorg B, “Dynamic performance enhancement of microgrids by advanced sliding mode controller”, International Jounal of Electric Power Energy System, vol. 33, no. 4, pp. 1–7, 2011.

[141] Jordehi, Javadi, Catalao, “Dynamic Economic Load Dispatch in Isolated Microgrids with Particle Swarm Optimisation considering Demand Response,” 55th International Universities Power Engineering Conference (UPEC), pp. 1-5, 2020.

[142] Imtiaz, Cui, Zafar, “Economic Dispatch of Microgrid incorporating Demand Response using Dragonfly Algorithm,” IEEE International Conference on Advances in Electrical Engineering and Computer Applications (AEECA), pp. 59-68, 2021.

[143] Singh, Poddar, Ramalingam, Shanmugam, Kalam, “Investigation on Dynamic Economic Dispatch Problem of Microgrid using Cuckoo Search Algorithm – Grid connected and Island mode,” IEEE Region 10 Conference (TENCON), pp. 1886-1891, 2019.

[144] Jordehi, Javadi, Catalao, “Dynamic Economic Load Dispatch in Isolated Microgrids with Particle Swarm Optimisation considering Demand Response,”

55th International Universities Power Engineering Conference (UPEC), pp. 1-5, 2020.

[145] Xin-She Yang, "Firefly algorithms for multimodal optimization," Stochastic Algorithms: Foundation and Applications SAGA 2009, vol. 5792, pp. 169-178, 2009.

[146] D. Karaboga, "An Idea based on Honey Bee Swarm for Numerical Optimization," Erciyes University, Engineering Faculty, Computer Engineering Department.,Tech. Rep. TR06, pp. 1-10,2005.

Appendix

List of Symbols

Symbol Definition

Chapter 3

Indices:

i	Units of generation.
n	Number of generation units.
avg	Average.

Parameters:

P	Total power output of the generator.
a	Cost co-efficient.
b	Cost co-efficient.
c	Cost co-efficient.
P_D	Total load during transmission of power from generation units to loads.
P_{loss}	Total power loss during transmission of power from generation units to loads.
λ	Lagrange multiplier.
u_x	Lagrange multiplier.
u_y	Lagrange multiplier.
$\lambda*$	Optimal incremental cost.
c_{12}	Communication link.
c_{21}	Communication link.
c_{23}	Communication link.
c_{32}	Communication link.
c_{34}	Communication link.
c_{43}	Communication link.
X[k]	Incremental cost of units at kth iteration.
μ[k]	Recursive step size.
G	r×r diagonal matrix with link control gain as its diagonal elements.
H_1, H_2	r×n matrix in which rows are elementary vectors.
D[k]	Noise in the communication link.
$X_{avg}[k+1]$	Set points for incremental costs of units.

Variables:

CP	Cost of generator.

P^{min}	Minimum generation limit of generator.
P^{max}	Maximum generation limit of generator.
IC	Incremental cost.
X[k+1]	Incremental cost of units at (k+1)th iteration

Chapter 4

Indices:

abc	Three-phase.
ref	Reference.
v	System.
g	Grid side.
o	Output.
1	Reactive power adjustment.
2	Terminal voltage adjustment.
PV	Photovoltaic.
ST	Steam Turbine.
STATCOM	Static Synchronous compensator/condenser.
L	Load.
IG	Doubly-fed induction generator.

Sets:

B	Set of BES technologies.
N	Set of depth of discharge segments.
G	Set of dispatchable units.
W	Set of renewable generation units.

Parameters:

$\dot{E}$	Virtual excitation electromotive force of VSG.
$\Delta\dot{U}$	Virtual synchronous impedance voltage drop.
I_O	Vector multiplication is performed to obtain ΔU.
r_a	VSG armature resistance.
X_d	Synchronous reactance.
J	Moment of inertia.
P_m	Mechanical power.
P_e	Electromagnetic power.
D	Damping coefficient.
ω	Angular velocity.
ω_N	Rated angular velocity.
$d\theta$	Correction angle of grid connection control module
f	Frequency.
Δf	Frequency deviation.
k_P	Power-frequency coefficient.

Q	Reactive power.
ΔQ	Change in reactive power.
ΔV	Change in output voltage of microgrid.
ΔE	Electromotive force.
C	Capacitance
L	Inductance
$\frac{K_v}{1+sT_v}$	Derivative of different components' reactive output power with respect to time and voltage.
K_p	Proportional gain.
K_i	Integral gain.
IAE	Integral absolute error.
ISE	Integral square error.
$ISTE$	Integral square time error.
Φ	Phase angle.
A_0	Initial value of the parameter.
A_{1s}	Parameter value after standard strategy is stable.
A_{1n}	Parameter value after new strategy is stable.

Variables:

U_{refabc}	Three-phase reference voltage.
$\Delta\omega$	Virtual angular velocity difference.
dE	Corrected electromotive force of the grid-connected control.
D_{1-0}	Difference offset ratio.
D_{n-s}	Parameter optimization degree of the new strategy relative to the standard strategy.